nature biomedical engineering

Article

https://doi.org/10.1038/s41551-022-01001-1

Ultrasensitive lateral-flow assays via plasmonically active antibody-conjugated fluorescent nanoparticles

In the format provided by the authors and unedited

Contents

Synthesis of plasmonically active core, gold nanorods:

To prepare plasmonic-fluor specific to 800CW dye, first AuNRs with absorbance wavelength 760 nm (localized surface-plasmon resonance wavelength ~760 nm) were synthesized by the seed-mediated method.[1] If needed, the wavelength of gold nanorods can be easily tuned to couple with different dye molecules to achieve the best enhancement factor. Briefly, to a solution of 9.75 ml 0.1 M hexadecyltrimethylammonium bromide (CTAB) (Sigma Aldrich, H5882), 0.25 ml 10 mM $HAuCl_4$ (Sigma Aldrich, 520918) and ice-cold 0.6 ml 10 mM $NaBH_4$ solution (Sigma Aldrich, 71321) was added under vigorous stirring at room temperature for 5 minutes or until the solution color changed to brown from yellow indication reduction of gold salt and formation of gold seed. Next to synthesize gold nanorods, 380 ml 0.1 M CTAB, 20 ml 0.01 M $HAuCl_4$ aqueous solution, 5.5 ml 0.01 M $AgNO_3$ (Sigma Aldrich, 20439 0), 8 ml 1 M HCl (Sigma Aldrich, H9892), 2.2 ml 0.1 M ascorbic acid (Sigma Aldrich, A92902) and 5 μl of seed solution were added sequentially. Each addition is followed by gentle homogenization and after last addition the subsequent solution is left in dark for 24 h. Finally, the solution was centrifuged at 7,000 rpm for 30 mins to remove excess reactants and was then reconstituted in nanopure water for further use.

Conjugation procedures (800CW-BSA-Biotin)

Using EDC–NHS chemistry, first BSA was conjugated with biotin. For this, solution of 2.2 ml 5 mg ml^{-1} BSA (Sigma Aldrich, A7030) in 1X PBS and 2 mg NHS–PEG4–biotin (Thermo Scientific, 21329) was incubated at room temperature for 1 h. BSA-biotin conjugates were purified by a desalting column (Thermo Scientific, 21329, 7,000 MWCO). Next, to conjugate 800CW to BSA-biotin, 100 μl 1M of K_2HPO_4 buffer (to raise pH of the solution to 9) was added to 1 ml of purified BSA-biotin solution. Subsequently, 25 μl of 4 mg ml^{-1} NHS–800CW (LI-COR, 929–70020) was added to the above solution, and incubated at room temperature for 2 h. Finally, conjugated BSA–biotin–800CW was purified using a Zeba desalting column pre-equilibrated with nanopure water.

Synthesis of plasmonic-fluor

Plasmonic-fluors were synthesized following the similar procedure described in our previous study.[2] AuNR (760 nm) was employed as the nanoantenna to prepare plasmonic fluor–800CW. 1 μl of (3-mercaptopropyl)trimethoxysilane (MPTMS) (Sigma Aldrich, 175617) and 1 ml of AuNR (extinction ~2) were mixed and shaken on rocking bed for 1 h. Next, 2 μl of APTMS (Sigma Aldrich, 281778) and 2 μl of trimethoxy(propyl)silane (TMPS) (Sigma Aldrich, 662275) was added to the MPTMS-modified AuNR to form the polymer spacer layer. Excess monomers were removed from the AuNR–polymer solution by two centrifugations at 6000 rpm for 10 min. After each wash the pellet was redispersed in 1 M CTAB aqueous solution. Polymer coated AuNRs were concentrated into a final volume of 10 μl. Next, to conjugate 800CW-BSA-Biotin complex to polymer modified AuNRs, we followed procedures mentioned in previously reported study.[3] Briefly, to allow coating of 800CW-BSA-Biotin to AuNRs, the pH of 100 μl 4 mg ml^{-1} BSA–biotin–800CW was lowered by adding 1 μl of 20 mg ml^{-1} citric acid (Alfa Aesar, 36664). To this solution, concentrated AuNR-polymer solution was added, and the resulting solution was sonicated for 20 min in dark. After coating, excess 800CW-BSA-Biotin was removed by centrifugation at 3,000 rpm for 10 min and incubated with 0.4 mg ml^{-1} of 800CW-BSA-Biotin in pH 10 nanopure water (1 μl NaOH in 10 ml of water) for 3 d at 4 °C. Finally, the nanostructures were washed 4 times using ph10 nanopure water by centrifugation at 3,000 rpm for 10 mins. Finally, nanolabels were redispersed in 1% BSA in 1X PBS solution for use in immunoassays.

Concentration measurements of nanolabels

The concentration of AuNPs and plasmonic-fluors were determined according to Beer's law: $A = \varepsilon \cdot c \cdot l$. Here, *A* is the local surface plasma resonance (LSPR) absorbance of nanolabels measured by UV-VIS spectroscopy, c is the concentration of nanolabels, l is the light path length (cm), ε is the molar extinction coefficient (M^{-1}□cm^{-1}) of nanoparticles described below: $10^{(1.0643*\log(1.5*3.14159*\text{diameter})+4.0935)}$.

Fluorescence enhancement of 800CW–streptavidin using AuNR–plasmonic-fluor–800CW:
The schematic of procedure adopted for the test is depicted in **Supplementary Fig. 43**. Specifically, first 100 μl of 50 ng ml^{-1} of BSA–biotin (in 1X PBS) was incubated at room temperature for 15 min. The wells were washed three times with 350 μl of PBST (0.05% Tween 20 in 1X PBS) followed by blocking with 300 μl of reagent diluent (1X PBS containing 3% BSA, 0.2 μm filtered). Next the wells were incubated with 1 μg ml^{-1} of streptavidin–800CW (LI-COR, 926-32230), diluted in reagent diluent, for 10 min. The wells were washed again with PBST and incubated with just PBS (for control) and 76 pM plasmonic-fluor in reagent diluent for

30 min. To remove unbound or excess plasmonic-fluors, the wells were washed again thrice with PBST. Subsequently, the fluorescence signal of well with and without plasmonic-fluors were measured using the LI-COR CLx fluorescence imager with the following scanning parameters: laser power ~L2; resolution ~169 μm; channel 800; height 4 mm.

Human IL-6 enzyme-linked immunosorbent immunoassay:
Human IL-6 ELISA was carried out according to the procedure mentioned in DuoSet ELISA kit manual. Specifically, wells were first coated with 100 μl 2 μg ml^{-1} (in 1X PBS) of capture antibodies via overnight incubation at room temperature. Next for blocking, 300 μl of reagent diluent (1X PBS containing 3% BSA, 0.2 μm filtered) was incubated in wells for minimum of 1 h. Next, 100 μl of serially diluted standard samples were incubated for 2 h, followed by incubation of 100 μl 50 ng ml^{-1} biotinylated detection antibodies for 2 h. Next, 100 μl of streptavidin labelled horseradish peroxidase (200-fold diluted using reagent diluent) was incubated for 20 min, followed by incubation of 100 μl of substrate solution, 1:1 mixture of color reagent A (H_2O_2) and B (tetramethylbenzidine) (R&D Systems, DY999) for 20 min. The reaction was stopped by addition of 50 μl 2N H_2SO_4 (R&D Systems, DY994) and immediately after the optical density at 450 nm was measured using a microplate reader.

Biotinylation of anti-human IgG:
Using EDC–NHS chemistry, antibodies were conjugated with biotin. First NHS-PEG4-biotin solution was prepared by addition of 170 μl of nanopure water in 2 mg of NHS-PEG4-biotin (Thermo Scientific, 21329). Next, mixture of 1 ml 2 mg ml^{-1} of anti-human IgG (Rockland, 609-4617) in 1X PBS and 30 μl NHS-PEG4-biotin solution were incubated at room temperature for 1 h. Biotinylated anti-human IgG was purified by 7,000 MWCO desalting column (Thermo Scientific, 21329).

Biotinylation of N protein detection antibody:
Using EDC–NHS chemistry, N protein detection antibodies were conjugated with biotin. First NHS-PEG4-biotin solution was prepared by addition of 170 μl of nanopure water in 2 mg of NHS-PEG4-biotin (Thermo Scientific, 21329). Next, mixture of 400 μl of as received N protein detection antibody (SinoBiologicals, 40143-R004) in 1X PBS and 5 μl NHS-PEG4-biotin solution were incubated at room temperature for 1 h. Biotinylated N protein detection antibody was purified by 7,000 MWCO desalting column.

Antibody conjugation on plasmonic-fluor:
Streptavidin-conjugated plasmonic-fluor (40 μl, extinction 32) was added to 50 μl of 4.5 μg/ml biotinylated anti-human IgG and biotinylated detection antibody for N protein at room temperature. The solution was incubated for 0.5 h and washed thrice with pH 10 water. For washing conjugated plasmonic-fluor was centrifuged at 6,000 rpm (2800 g) for 10 minutes. Finally, the pellet was resuspended in 1% BSA in 1x PBS and stored in 4 C for further use in immunoassays.

RMC calculations:
The RMC is a recently introduced bioanalytical parameter that helps in determining whether the signal of an unknown concentration μx can be distinguished from the signal of a certain concentration, x, at a certain confidence level for a 2-sided t-test.[4] A molecular assay can be considered 'good' if it can resolve <100% changes in the concentration of analyte along a clinically meaningful concentration range. In other words, the RMC (μ) should be below 2 over the desired concentration range.[4] In our case, we defaulted to the 99% confidence interval to determine the range of concentration for which μ is below 2. This stringent criteria in determining the RMC of p-LFA helps us in identifying the working concentration of the p-LFA in a standard-free manner with 99% certainty.

For example, a μ value of 1.4511 at x = 2.47 pg/mL (**Supplementary Fig. 44**) would mean that at 2.47 pg/mL, p-LFA can distinguish 45.11% change (*i.e.* 2.47 to 3.58 pg/mL) in concentration with 99% confidence. Furthermore, since the concentration range over which $\mu < 2$ is 0.1292–86.08 pg/mL, IL-6 p-LFA can distinguish the signal corresponding to any two concentrations that differ by at least 100% within that range with at least 99% confidence. We also evaluated the $\mu < 5$ range (0.0281–180.979 pg/mL) because our dose responses were performed with 5-fold serial dilutions and this measurement gives another point of evaluation for comparison of assay performance of p-LFA, p-FLISA, and ELISA (**Supplementary Fig. 44**).

To calculate the RMC, we first fitted our dose response data with the following Langmuir Binding Isotherm function for a signal-on assay using OriginPro's function builder:

$$S(x) = (S_{max} - S_0)\frac{x}{x+K_D} + S_0$$

Next, we calculated the RMC values and parameters according to the equations mentioned below:[4]

$$\frac{Z}{\sqrt{3}} = \frac{|S(\mu x) - S(x)|}{\sqrt{(\sigma_{S(x)})^2 + (\sigma_{S(\mu x)})^2}}$$

where is determined via following error propagation equation:

$$\sigma_S = \sqrt{\sum_{i=1}^{n} \left(\frac{\partial S}{\partial c_i}\sigma_{c_i}\right)^2}$$, where $c_i = \{S_{max}, S0, KD\}$

Z is the critical value and is equal to 4.604 for a 2-sided t-test with 4 degrees of freedom corresponding to a 99% confidence interval.

RMC calculations were then performed via Python3. Our code outputs an excel file with x (concentration in the same units as original dose response) values, their corresponding μ values with an insignificant ± 0.0008 units of uncertainty. The minimum μ value and the range where μ is under 2 and 5, are printed in the Python3 shell. The uncertainty in μ comes from how our code solves the RMC equation implicitly by incrementing μ by 0.0004 units to estimate what μ value equals the constant on the left side of the equation. NumPy[5] and Matplotlib[6] packages were used to aid these calculations. The Python3 Code for RMC can be found at https://github.com/seanwangsalad/PythonRMC.

Data processing on the data acquired by portable scanner:
The portable fluorescence scanner outputs each data point in the form of the average pixel value (signal intensity) versus the travel length of LFA strip through the scanner by 100 μm increments. Subsequently, Python3 was used to perform baseline correction, a process that normalizes the data and separates the true fluorescence signals from the background noise. This correction was performed by using the iModPoly algorithm[7] followed by another correction with the Mixture Model algorithm[8], which were both provided in the pybaselines package (*GitHub Repository: https://github.com/derb12/pybaselines)*. For ease of data processing, the first 25 data points were truncated as the test/control lines were printed from x=60 to 150 (6 to 15 mm). Truncated regions are represented with 0 signal intensity. For example, in **Supplementary Fig. 32**, the region of 0-2.5 or 0-25 data points were set to 0.

After baseline correction, relevant/key local minima and maxima were calculated. Since the test line was printed at around 11 mm along the LFA strip, the largest maxima nearest to this point is chosen as the signal's apex. Subsequently, 2 local minima based on the mean of the pairs that were closest to that maximum were chosen. The centroid of these 3 points estimates the center of the test line's signal area. These calculations were aided by NumPy[5] and SciPy packages[9]. In addition, Matplotlib was used to generate all representations.[6]

Data processing for LFA strip drop-casted with known concentrations of nanolabels

To find the total signal produced by the test line, integration of the signal intensity curve within a range of ±2.5mm (plasmonic-fluor) or ±2.0mm (molecular fluorophore, 800CW) from the centroid was implemented. These ranges were determined by the range that the highest concentration of drop-casted nanolabels encompassed (**Supplementary Fig. 32 and 33**). For all further tests we used the same range for signal integration. As representative examples of data processing in **Supplementary Fig. 32 and 33** we show the original and corrected processed data for low and high concentrations, (~10^6 and ~ 10^3 for plasmonic-fluors and ~10^{11} and ~ 10^6 for molecular fluorophores) and blank data points corresponding to plasmonic-fluor and molecular fluorophore nanolabels, respectively.

Data processing for p-LFA strip subjected to standard target analyte

p-LFA strips contain both test line and fluorometric control line are expected to exhibit either one or two peaks: a positive reading will result in two peaks and a negative result would result in one peak occurring at the control line. In both cases, our code automatically truncates the data corresponding to the region where the control line is printed (x > 125 data points or > 12.5 mm) before baseline correction and integration. However, if a test were to have no signal at the control line, our code will report it as an invalid test result. As an example, please refer to **Supplementary Fig. 38 and 40** which show the above-described truncation process of the data acquired from p-LFA strip exposed to known concentration of IL-6 and N protein, respectively.

Data processing for p-LFA strip subjected to patient samples

Data processing for p-LFA strips subjected to patient samples use the same methods described above. However, due to the varying amount of non-specific proteins or debris in the patient samples, there may be varying background signal that can interfere with baseline correction. For example, in case of **Supplementary Fig. 42**, if there is signal downstream of the test line that is greater than 50% of the test line, the code will truncate the region after the printed test line ($x > 125$ data points or > 12.5 mm) before baseline correction and integration as shown in **Supplementary Fig. 42**.

The code for the software can be found at:
https://github.com/seanwangsalad/AreaUnderCurveForLFAReader.

Supplementary figures

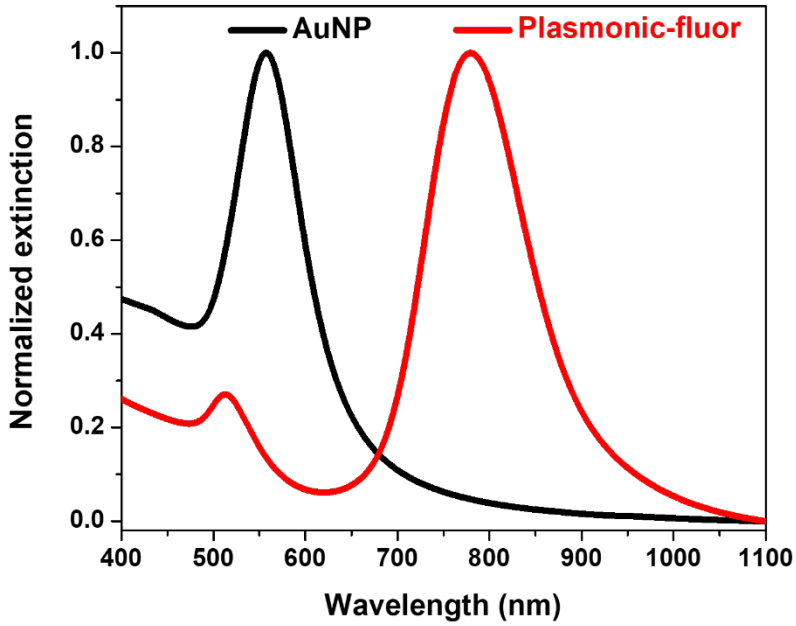

Supplementary Fig. 1 l Visible-NIR extinction spectra of streptavidin functionalized AuNPs (black) and plasmonic-fluors (red).

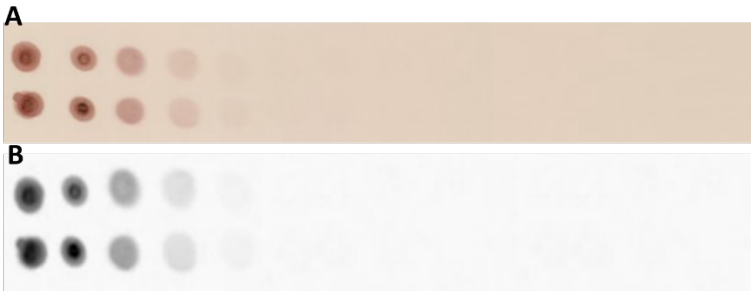

Supplementary Fig. 2 l (A) Digital photograph of a strip drop-casted with different concentrations of AuNPs. **(B)** 8-bit ImageJ processed image.

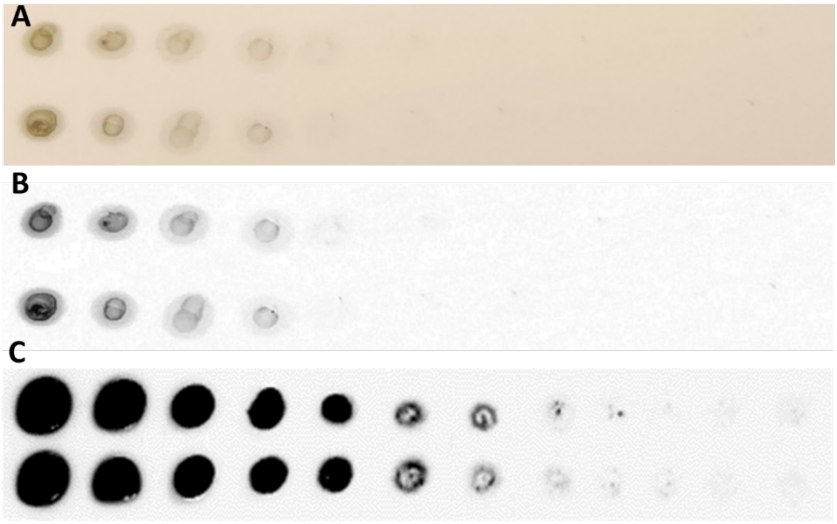

Supplementary Fig. 3 l (A) Digital photograph of the strip drop-casted with different concentrations of plasmonic-fluors. **(B)** 8-bit ImageJ processed image. **(C)** Corresponding fluorescence image of the nitrocellulose membrane.

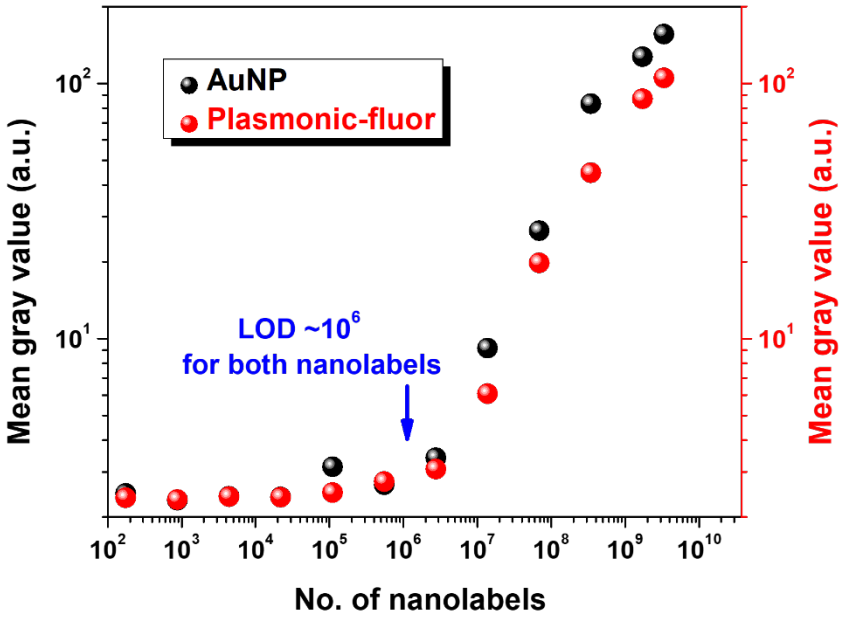

Supplementary Fig. 4 l Mean gray values obtained from nitrocellulose membrane drop-casted with different concentrations of AuNPs (black) and plasmonic-fluors (red).

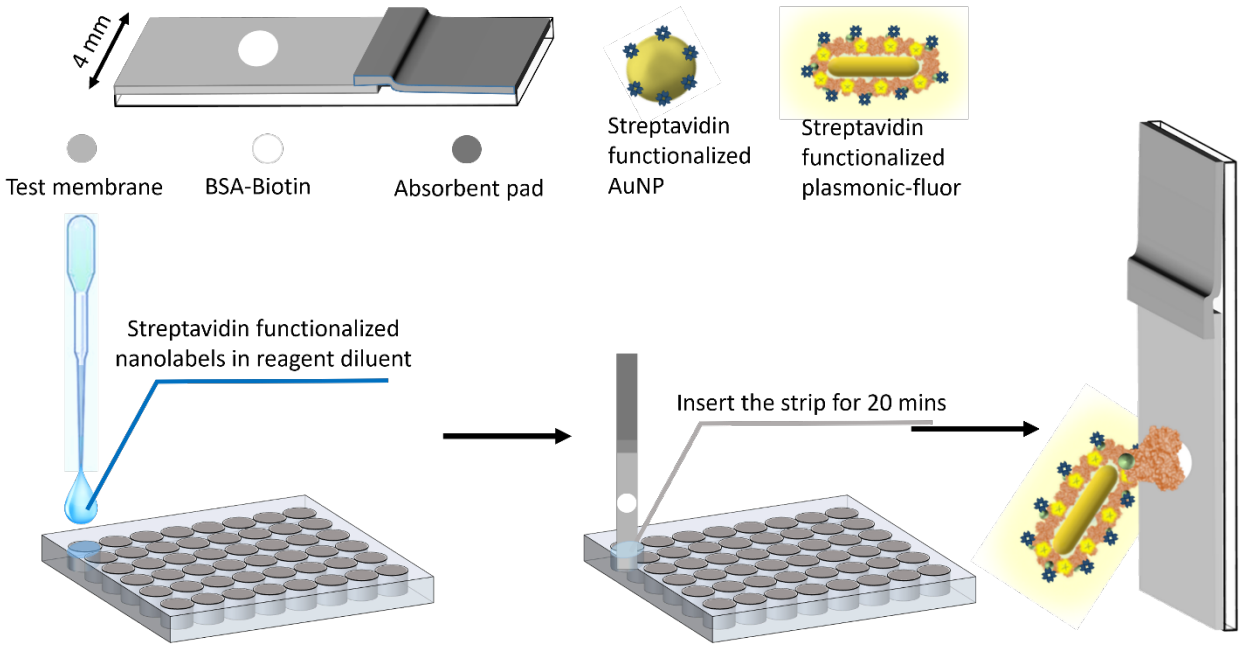

Supplementary Fig. 5 l Schematic representation of the experiment conducted to determine minimum concentration of nanolabels needed to produce detectable signal on nitrocellulose membrane in LFA format.

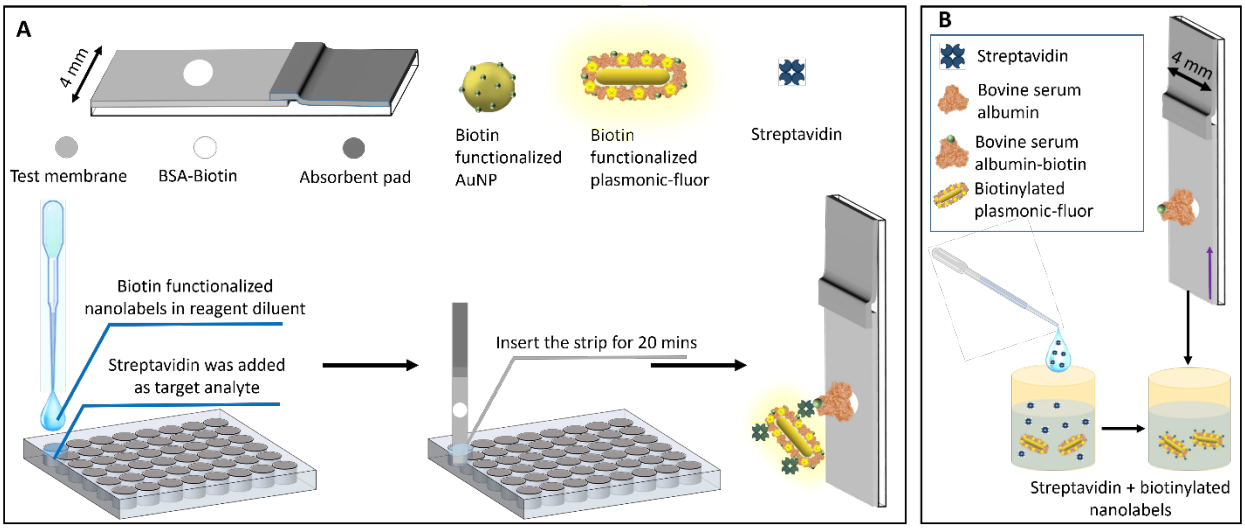

Supplementary Fig. 6 l Schematic representation of **(A)** biotin-streptavidin lateral flow assay and **(B)** corresponding work-flow of p-LFA.

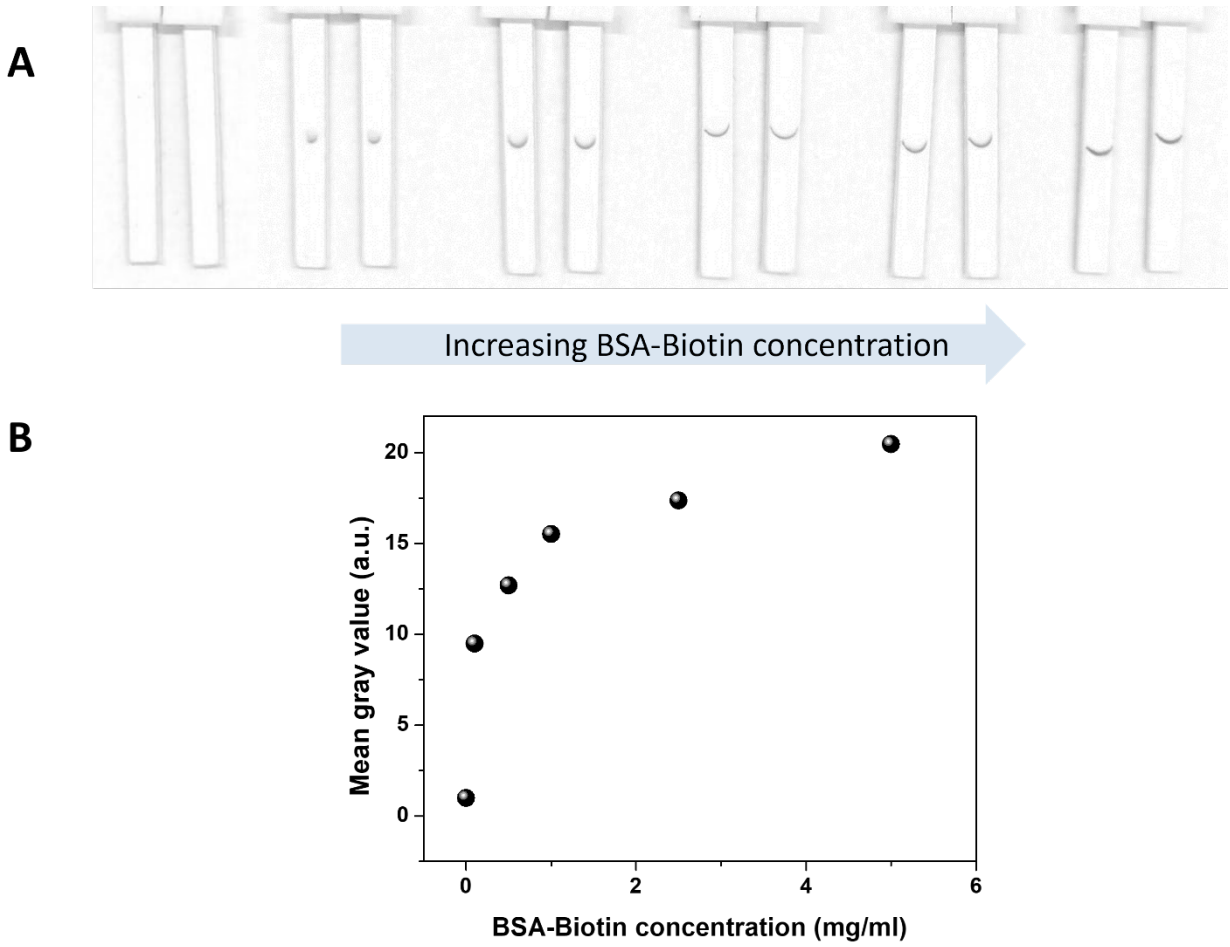

Supplementary Fig. 7 l (A) Image of the LFA strips (after Image J processing), with different concentrations of BSA-Biotin as capture spot, after exposure to the same concentration of streptavidin as target analyte and biotin-functionalized AuNPs. **(B)** Corresponding mean gray values as a function of BSA-Biotin concentration.

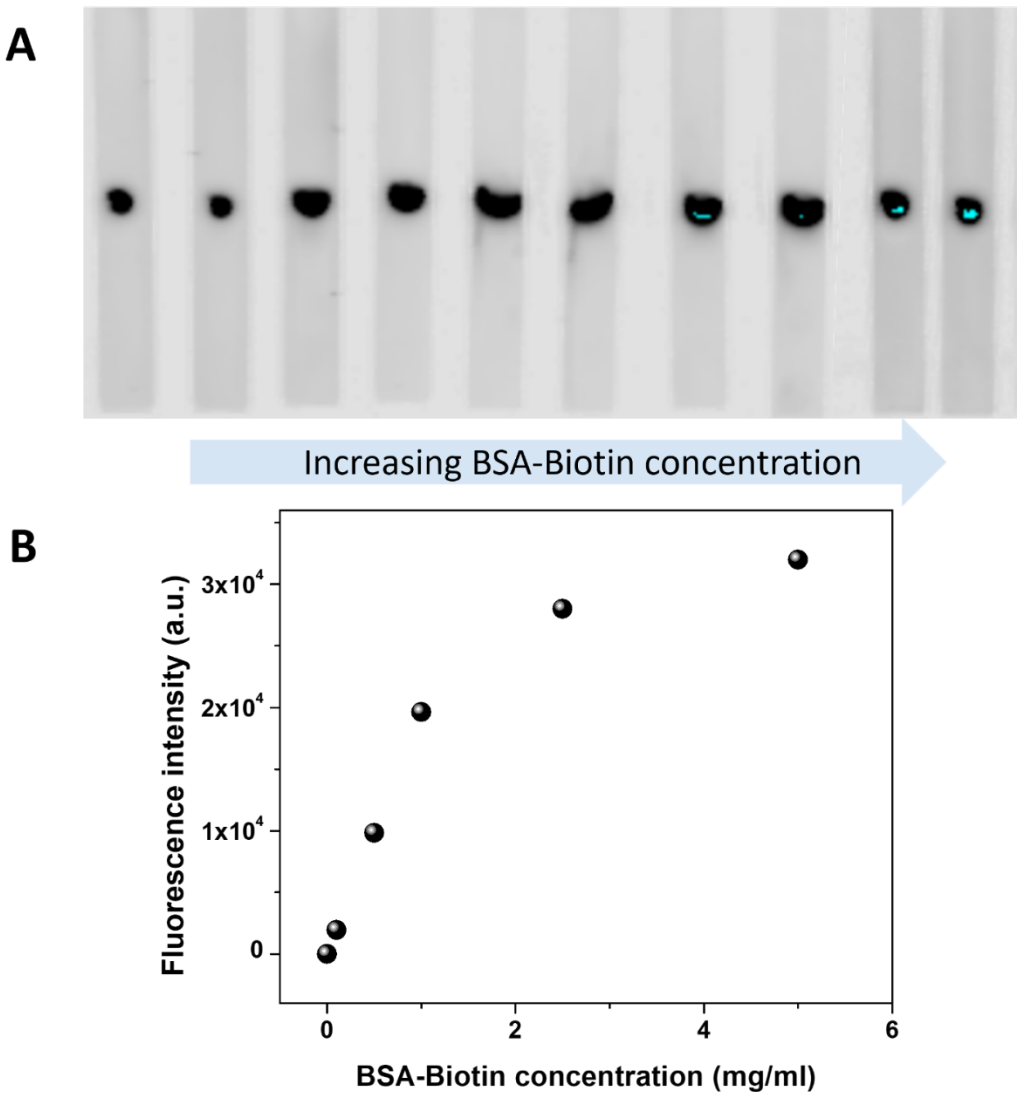

Supplementary Fig. 8 l (A) Fluorescence image of the LFA strips, with different concentrations of BSA-Biotin as capture spot, after exposure to the same concentration of streptavidin as target analyte and biotin-functionalized plasmonic-fluors. **(B)** Corresponding fluorescence intensity as a function of BSA-Biotin concentration.

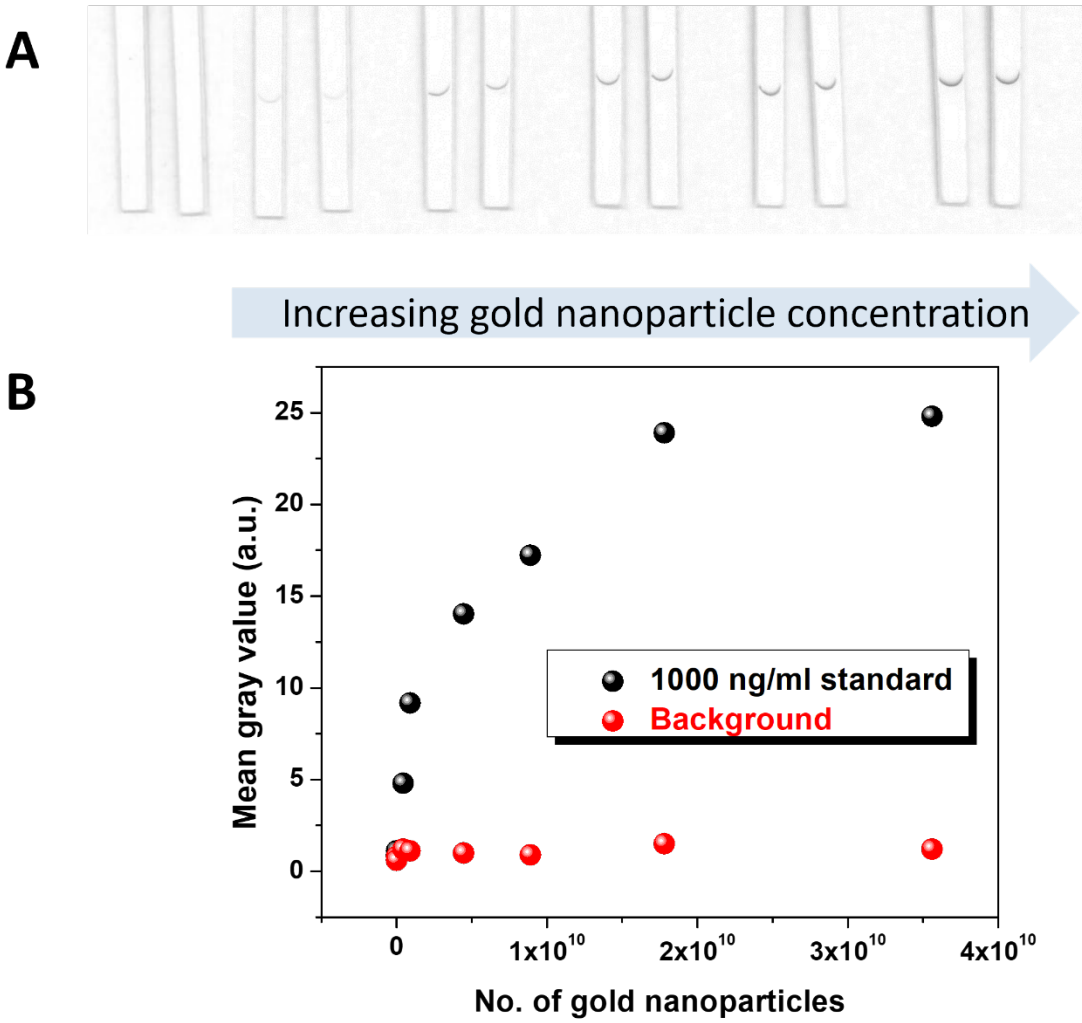

Supplementary Fig. 9 l (A) 8-bit ImageJ-processed image of the nitrocellulose membranes with the same concentration of BSA-Biotin concentration after exposure to different concentrations of biotin functionalized AuNPs, and identical concentrations of streptavidin as target analyte. **(B)** Corresponding mean gray values as a function of AuNP concentrations.

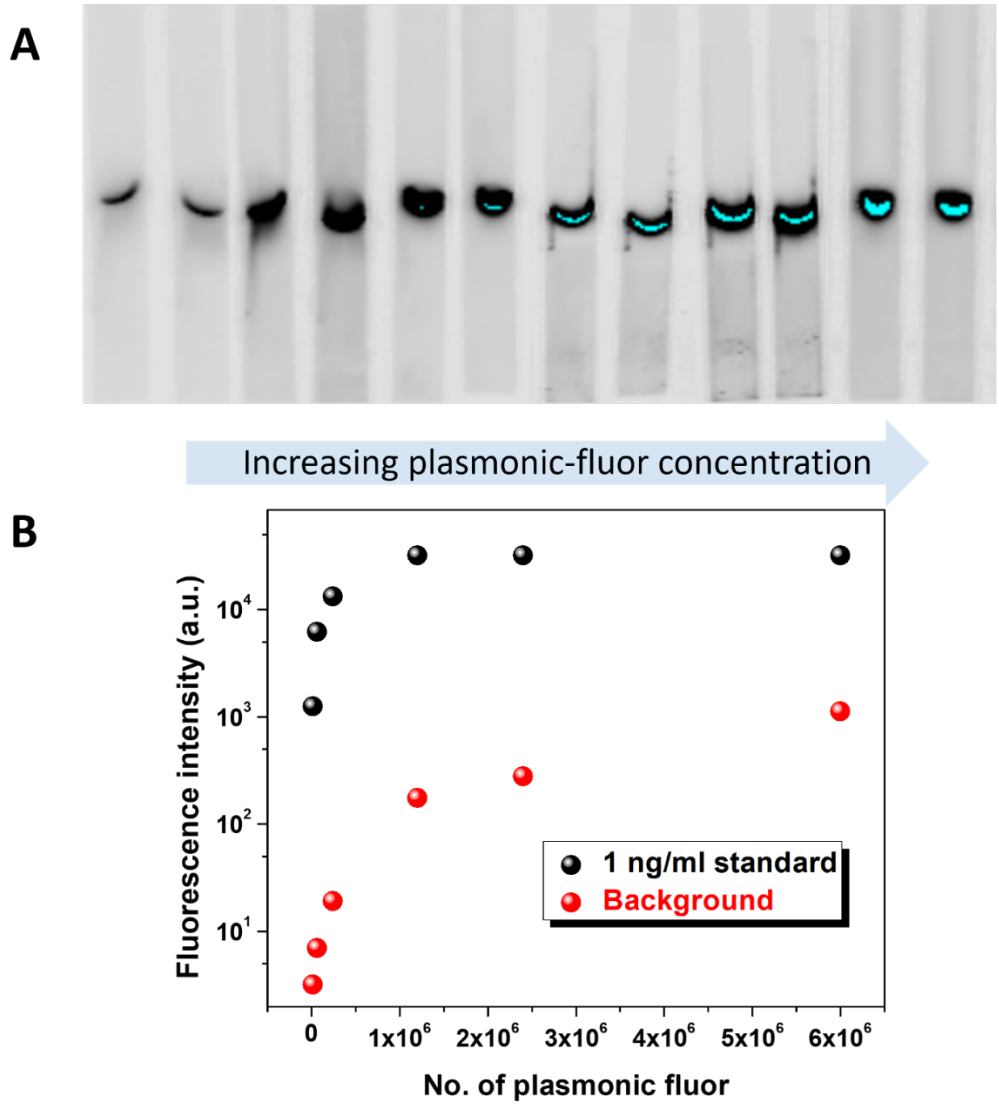

Supplementary Fig. 10 l (A) Fluorescence image of LFAs with the same concentration of BSA-Biotin concentration after exposure to different concentrations of biotin functionalized plasmonic-fluors, and identical concentrations of streptavidin as target analyte. (B) Corresponding fluorescence intensity as a function of plasmonic-fluors concentration.

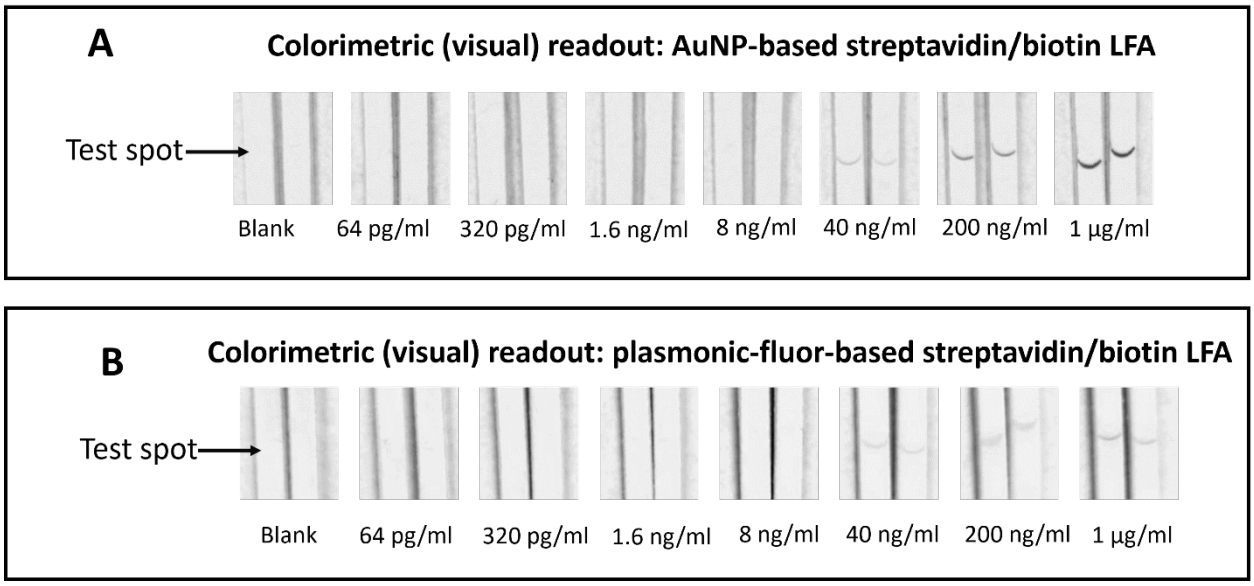

Supplementary Fig. 11 l 8-bit ImageJ processed images of nitrocellulose membranes corresponding to **(A)** AuNPs-based streptavidin-biotin LFA and **(B)** streptavidin-biotin p-LFA depicting the visual or colorimetric readout mode.

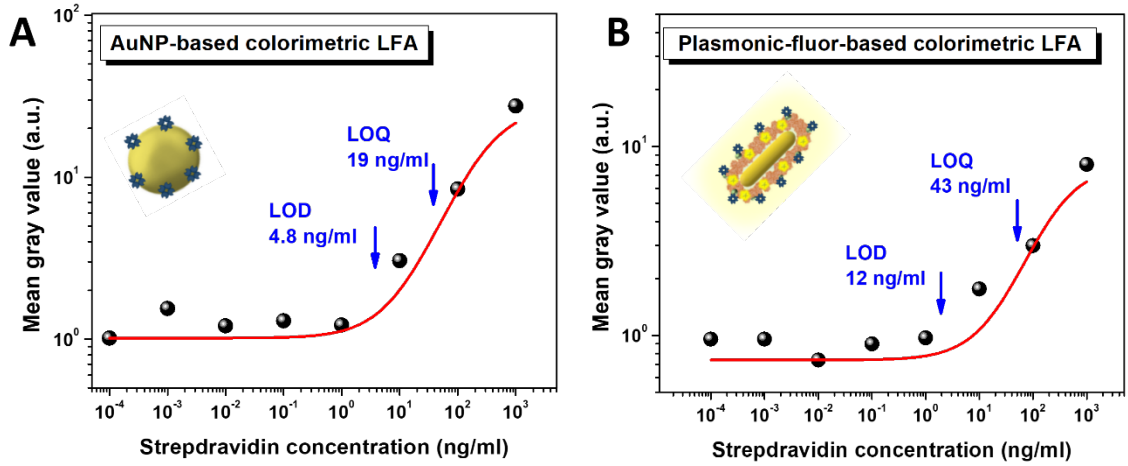

Supplementary Fig. 12 l Dose-dependent mean gray values obtained from nitrocellulose membrane corresponding to different concentrations of streptavidin acquired from **(A)** AuNP-based and **(B)** plasmonic-fluor-based biotin-streptavidin LFA.

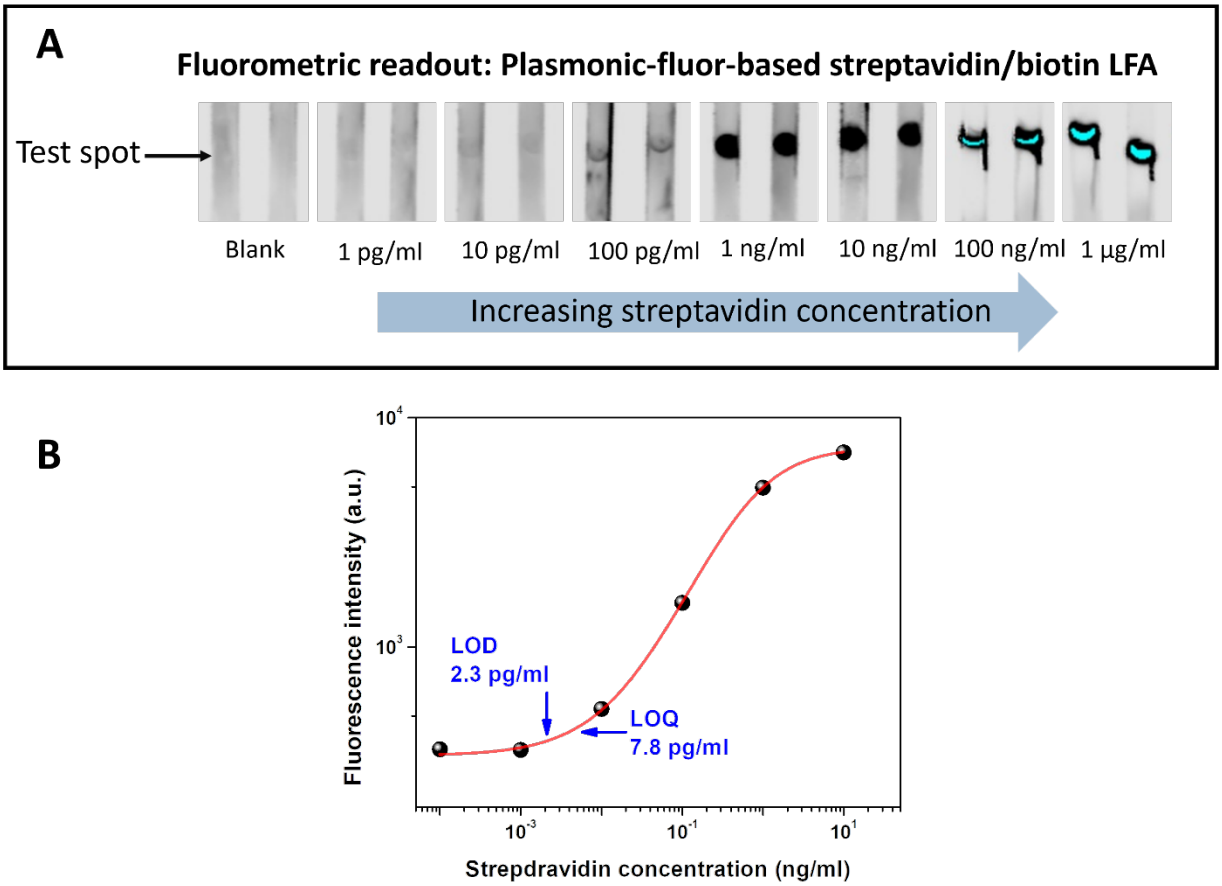

Supplementary Fig. 13 l (A) Fluorescence image of the nitrocellulose membranes corresponding to streptavidin-biotin p-LFA strips depicting fluorometric readout mode. **(B)** Dose-dependent mean gray values obtained from nitrocellulose membrane corresponding to different concentrations of streptavidin acquired from streptavidin-biotin p-LFA.

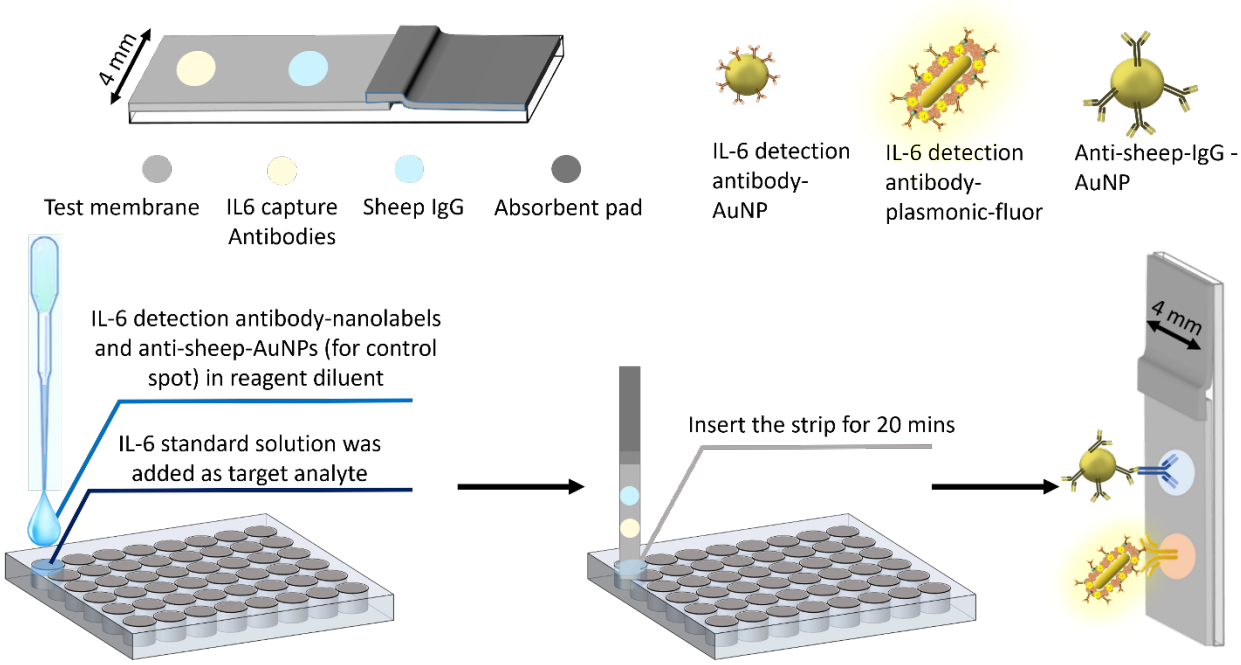

Supplementary Fig. 14 l Schematic representation of IL-6 plasmonic-fluor-based lateral flow assay.

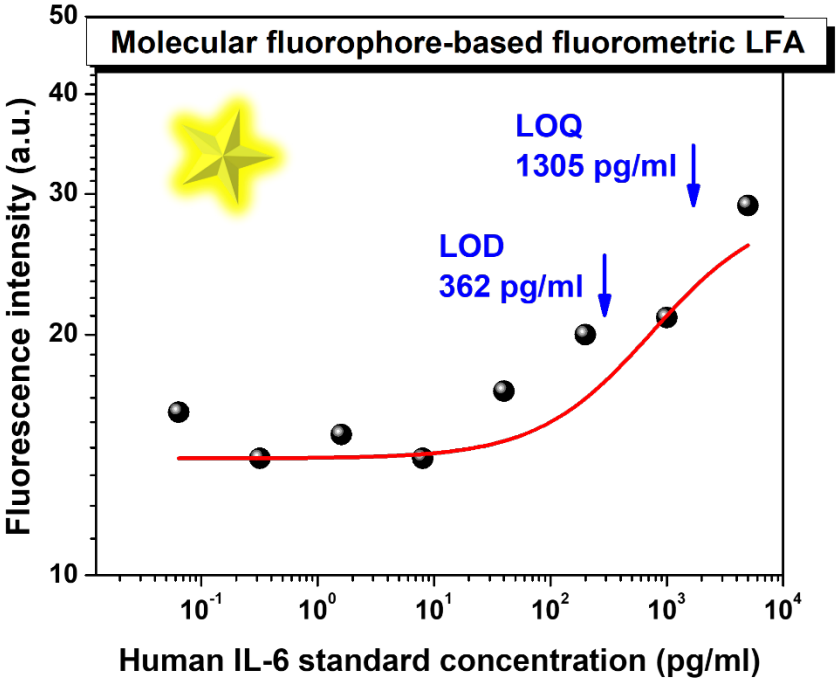

Supplementary Fig. 15 l Dose-dependent fluorescence intensity values obtained from nitrocellulose membrane corresponding to different concentrations of IL-6 standards acquired from molecular fluorophore-based LFA.

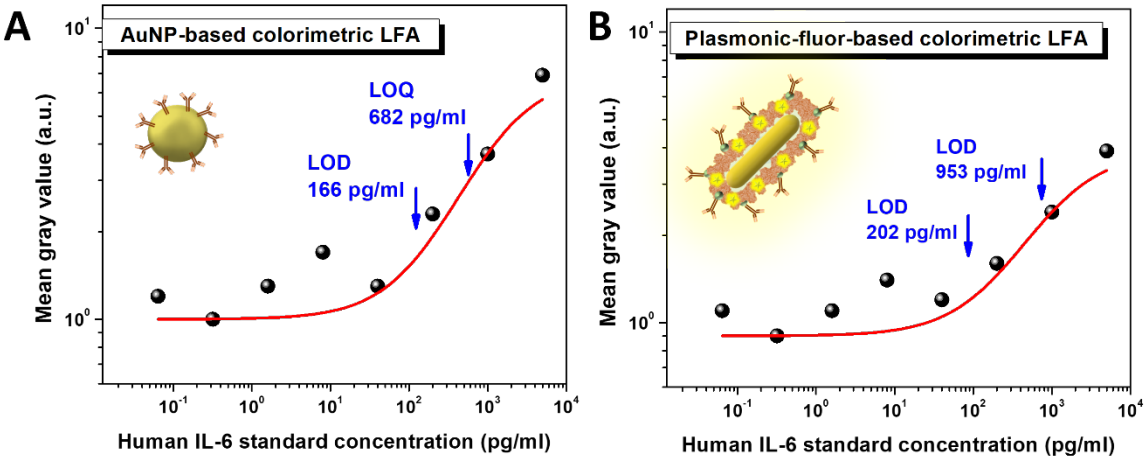

Supplementary Fig. 16 l Dose-dependent mean gray values obtained from nitrocellulose membrane corresponding to different concentrations of IL-6 standards acquired from **(A)** AuNP-based and **(B)** plasmonic-fluor-based IL-6 LFA.

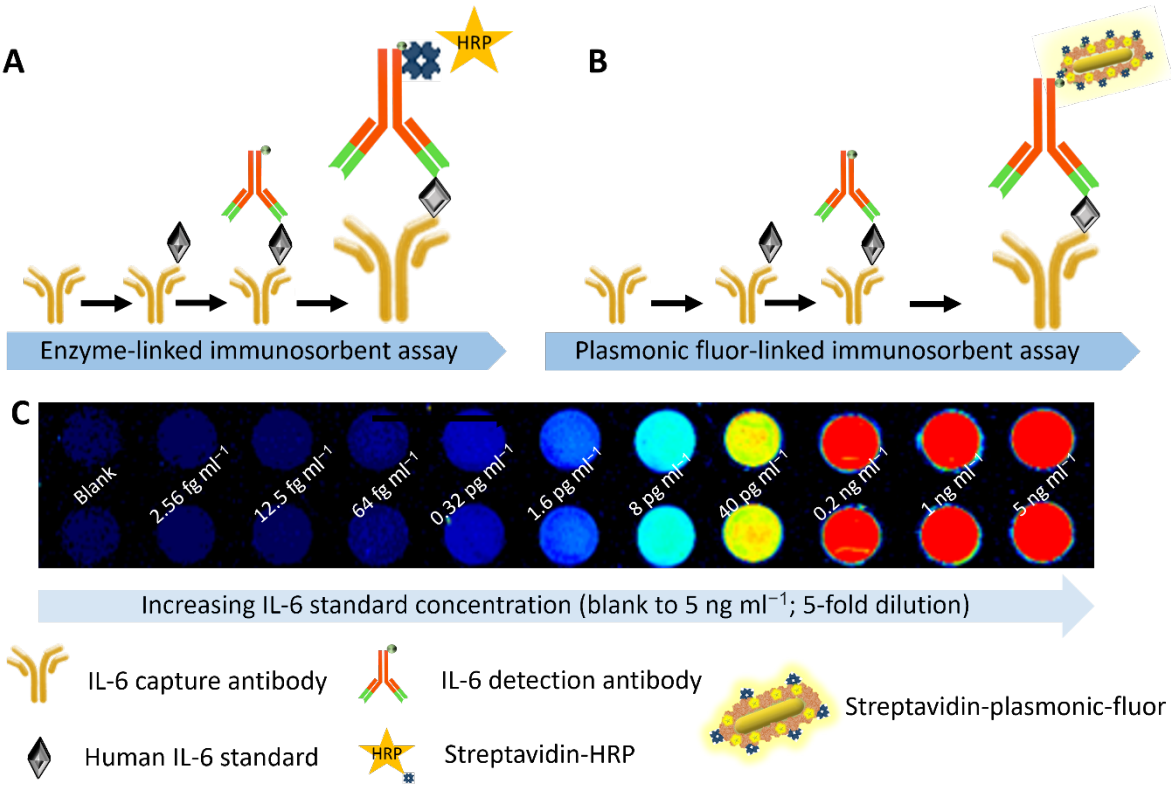

Supplementary Fig. 17 l Schematic representation of **(A)** ELISA and **(B)** p-FLISA. (Bottom) Dose-dependent fluorescence intensity maps acquired by p-FLISA for different IL-6 concentrations.

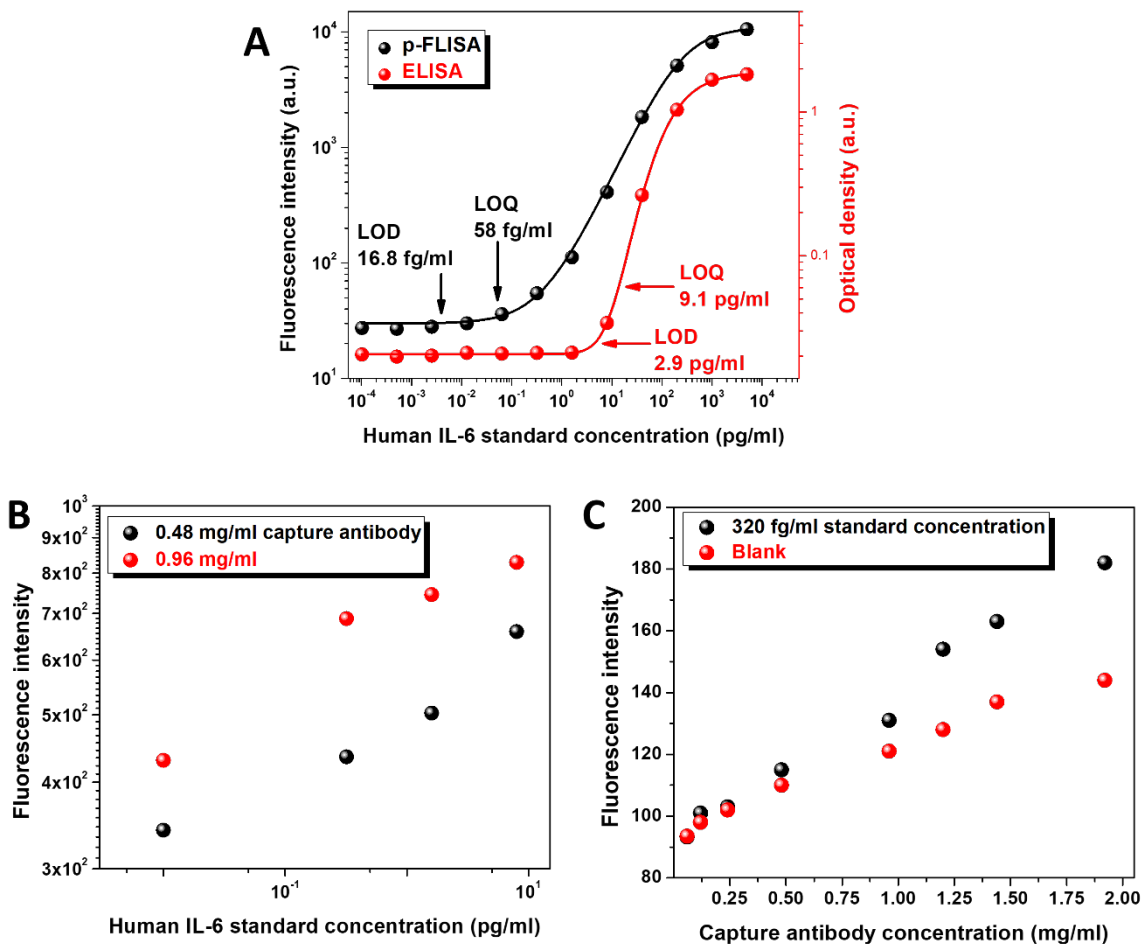

Supplementary Fig. 18 l (A) Dose-dependent fluorescence intensities and optical densities, corresponding to different IL-6 concentrations in plasmonic fluor-linked immunosorbent assay (p-FLISA, black circles) and standard ELISA (red circles), respectively, implemented on a microtiter plate, performed in 4 h. **(B)** Dose-dependent mean gray values obtained from nitrocellulose membrane corresponding to different concentrations of IL-6 standards acquired from IL-6 p-LFA strips drop-casted with different capture antibody concentrations. **(C)** Fluorescence intensity obtained for blank and 320 fg/ml human IL-6 standard concentrations from p-LFA strips as a function of capture antibody concentration.

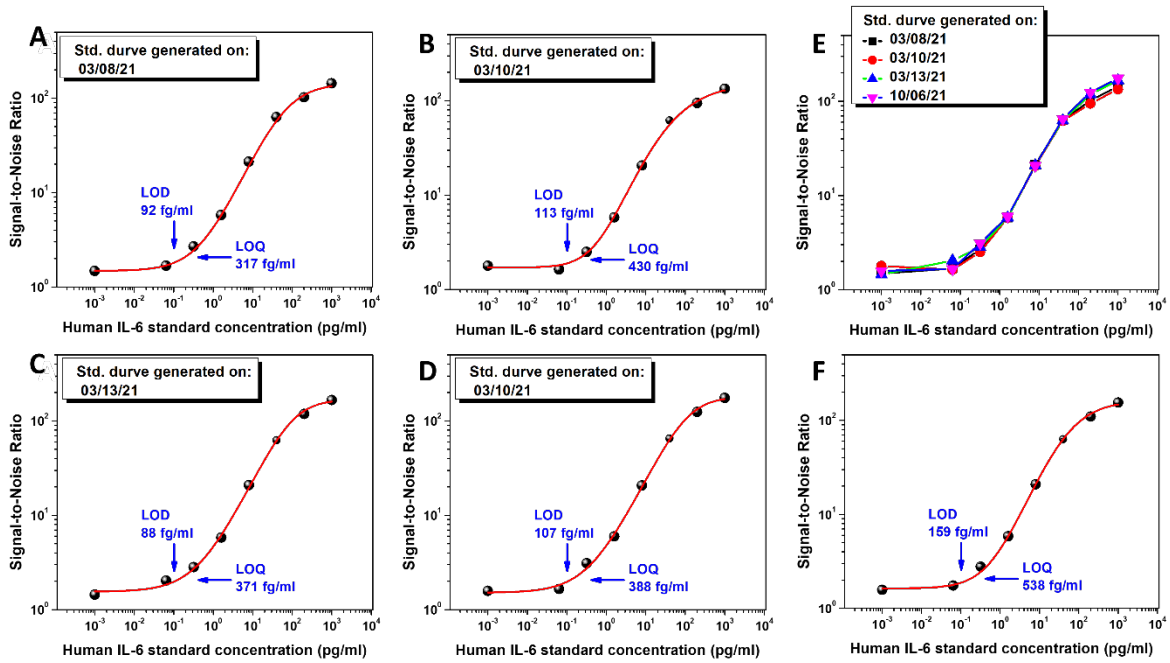

Supplementary Fig. 19 l (A-D) Dose-dependent signal-to-noise ratio of multiple IL-6 p-LFA standard curves generated on different dates. **(E)** Overlaid dose-dependent signal-to-noise ratio of different standard curves depicting minimal deviation from one another. **(F)** Dose-dependent signal-to-noise ratio obtained by taking the average values from all four standard curves and its bioanalytical parameters. Error bars in figure F represent standard deviations from 8 different samples.

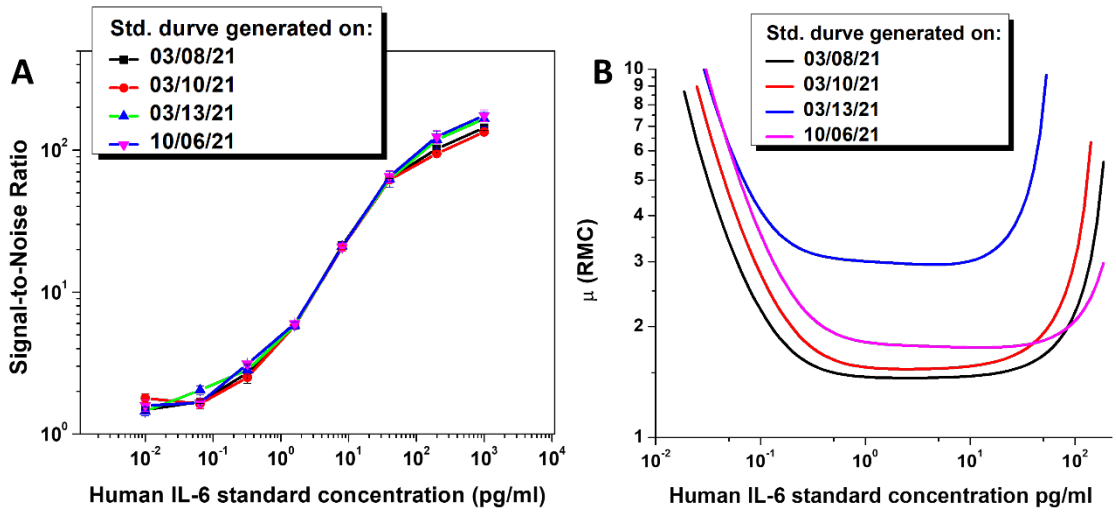

Supplementary Fig. 20 l (A) Overlaid dose-dependent signal-to-noise ratio of different standard curves depicting minimal deviation from one another. **(B)** Resolution of molecular concentration (RMC) curves for four different standard curves.

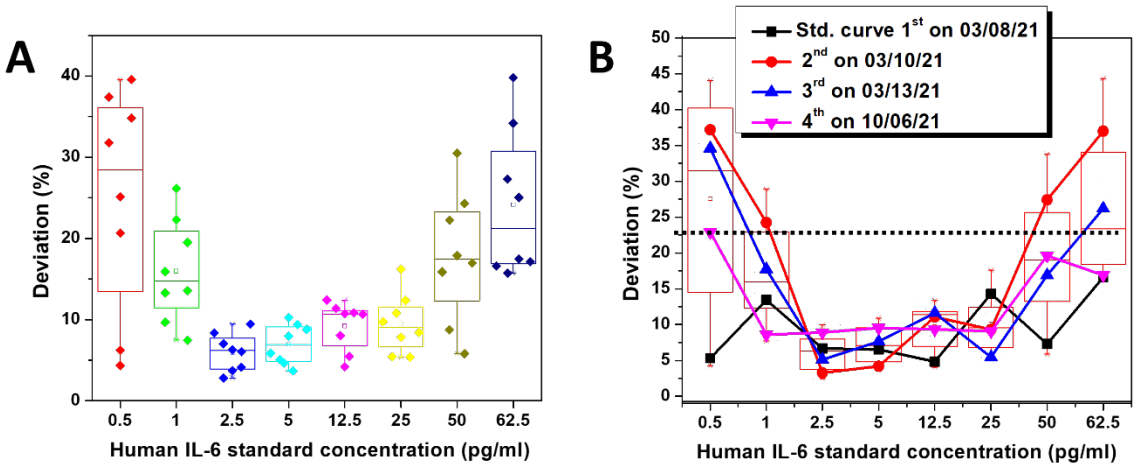

Supplementary Fig. 21 l Multiple IL-6 standard curves were generated and samples with varying IL-6 concentrations (0.5 pg ml⁻1 to 62.5 pg ml⁻¹) were tested in standard-free manner. Their experimental concentrations were determined using each standard curve, and deviation from actual concentration was calculated. **(A)** Samples were tested in duplicates in standard-free manner and for each test, experimental values were determined using 4 standard curves, thus, 8 data points corresponding to each concentration are plotted in the box plot. **(B)** Deviation in the average experimental values of the samples corresponding to each standard curve. Center line is median; center square is mean; box limits are first and third quartile which are 25% and 75% respectively; 1.5 times of interquartile range is defined by cross marks; the upper whisker is the first number that is less than upper quartile + 1.5 times of inter quartile range; Outliers are the data points located outside the 1.5 times of interquartile range.

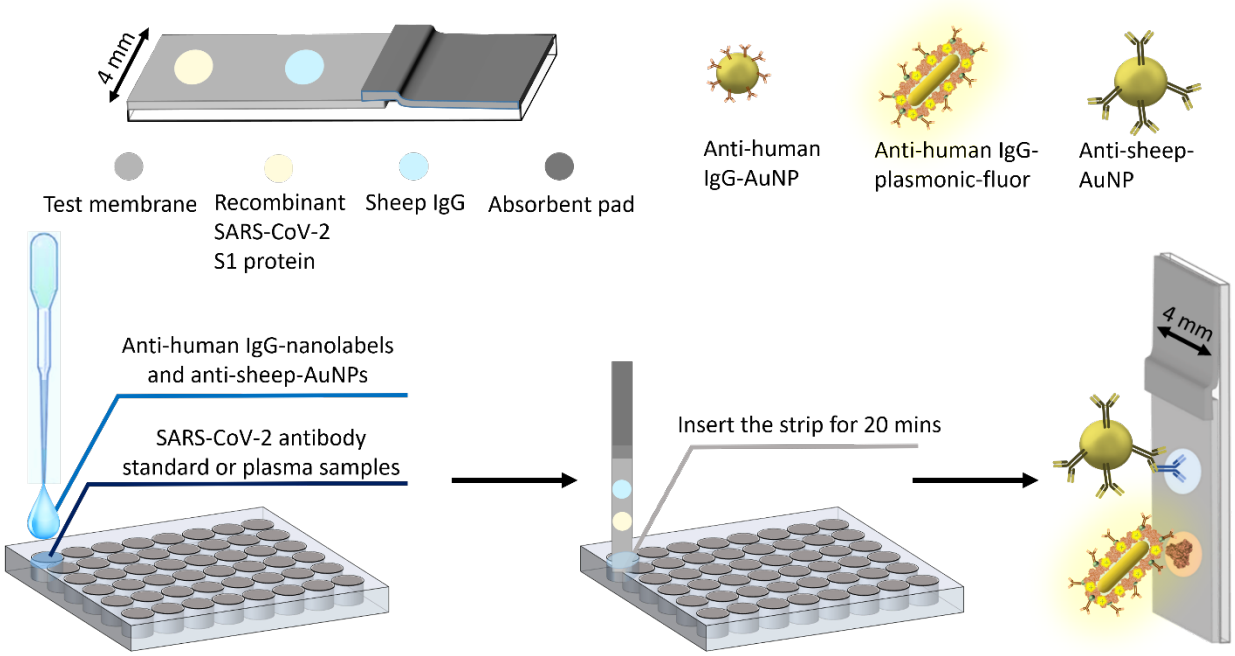

Supplementary Fig. 22 l Schematic representation of SARS-CoV-2 S1 plasmonic-fluor-based antibody lateral flow assay.

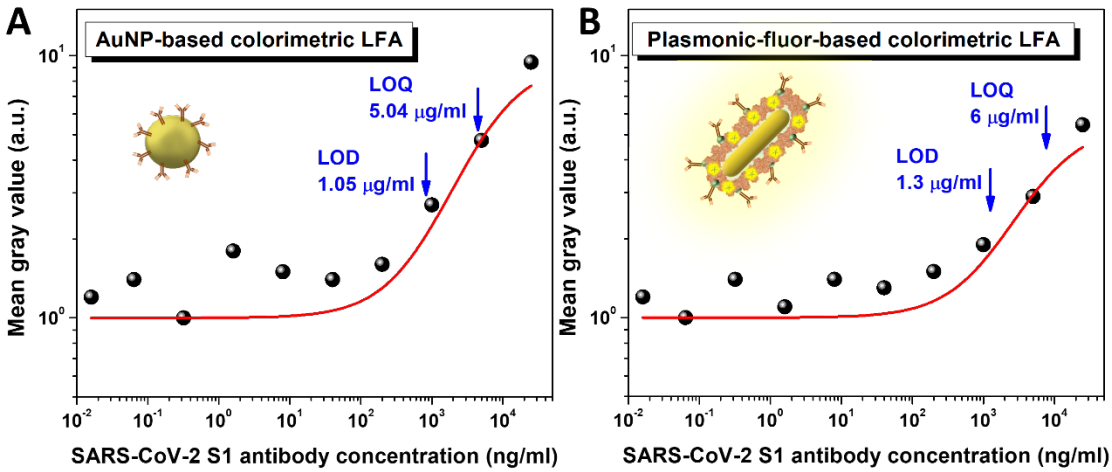

Supplementary Fig. 23 l Dose-dependent mean gray values obtained from nitrocellulose membrane corresponding to different concentrations of SARS-CoV-2 S1 antibody solutions acquired from **(A)** AuNP-based and **(B)** plasmonic-fluor-based SARS-CoV-2 antibody LFA.

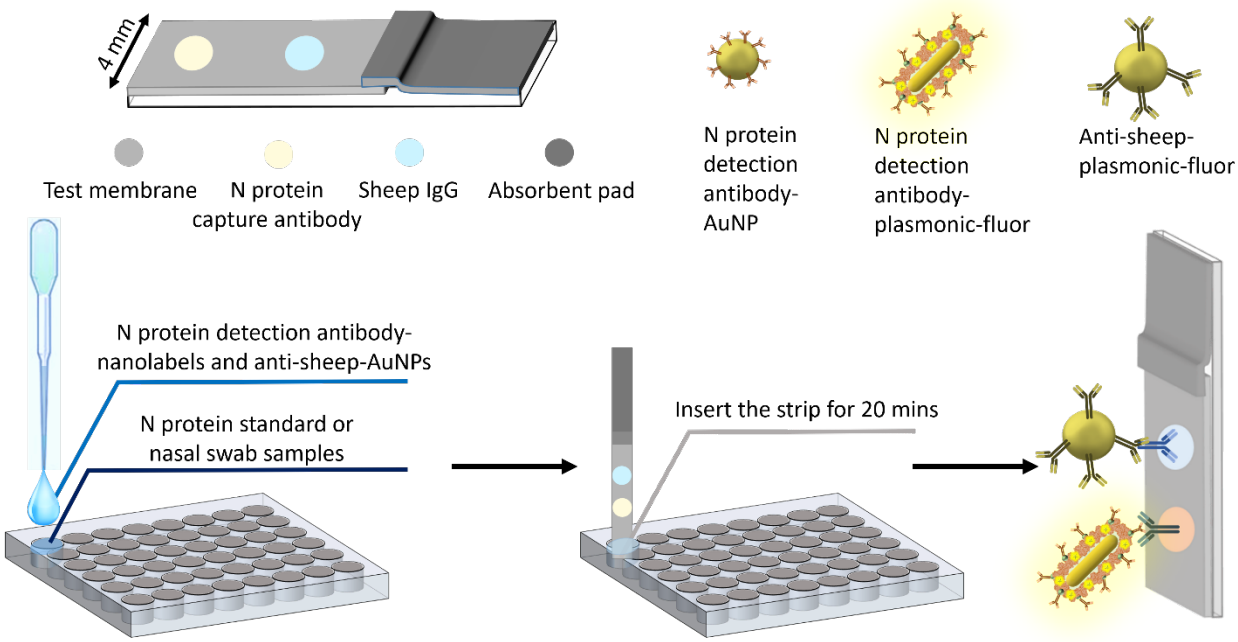

Supplementary Fig. 24 l Schematic representation of nucleocapsid protein plasmonic-fluor-based lateral flow assay.

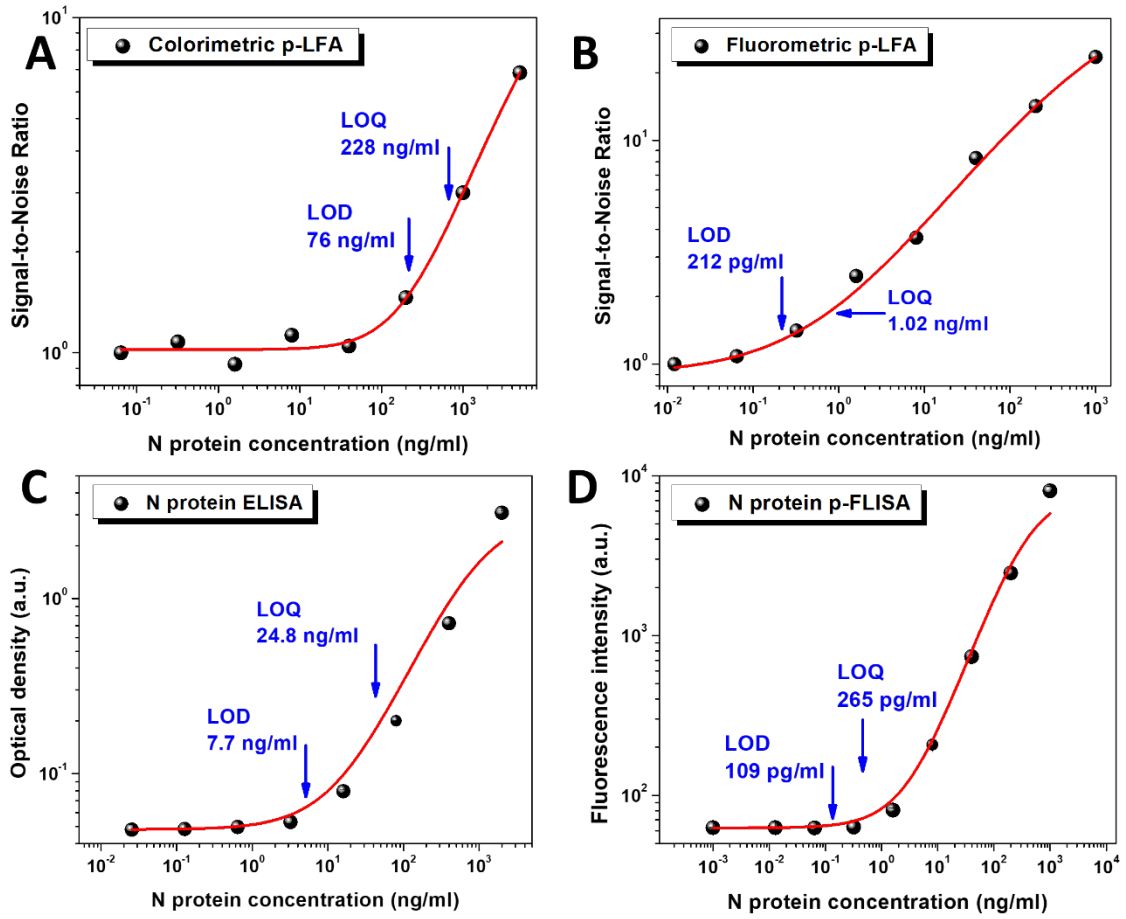

Supplementary Fig. 25 l Dose-dependent signal-to-noise ratio of **(A)** colorimetric and **(B)** fluorometric p-LFA for detection of N protein. **(C)** Dose-dependent optical density corresponding to different concentrations of N protein in ELISA. **(D)** Dose-dependent fluorescence intensity corresponding to different concentrations of N protein in plasmonic-fluor linked immunosorbent assay (p-FLISA). **(C and D)** Both the assays were implemented on microtiter plate and the sample-to-answer time was 4 h.

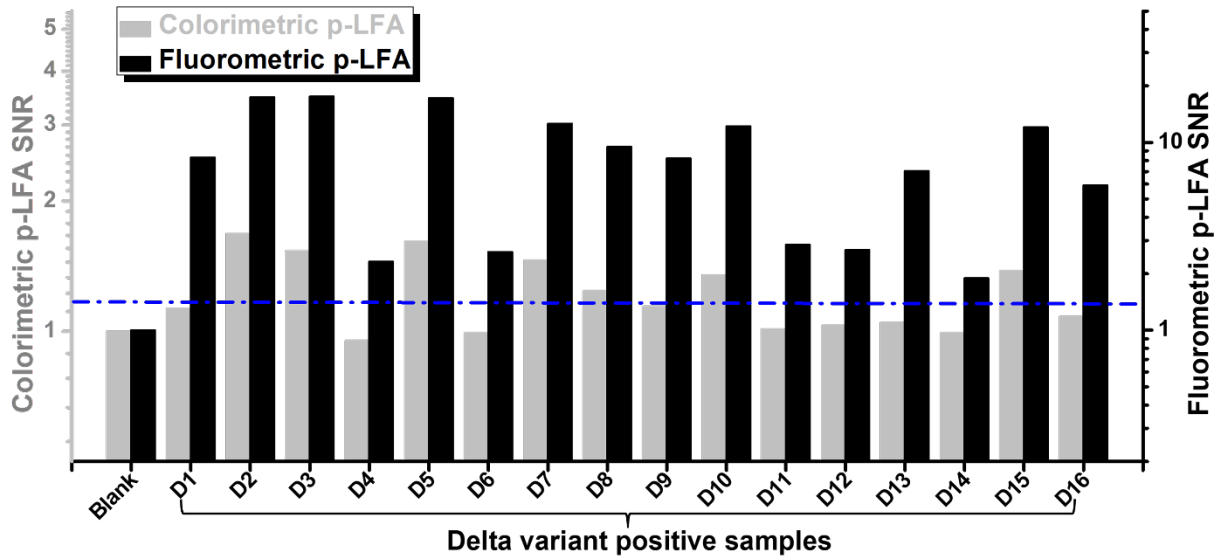

Supplementary Fig. 26 l N-protein signal-to-noise ratio in PCR-positive Delta B.1.617.2 variant NP swab samples determined by colorimetric p-LFA (gray bars) and fluorometric p-LFA (black bars).

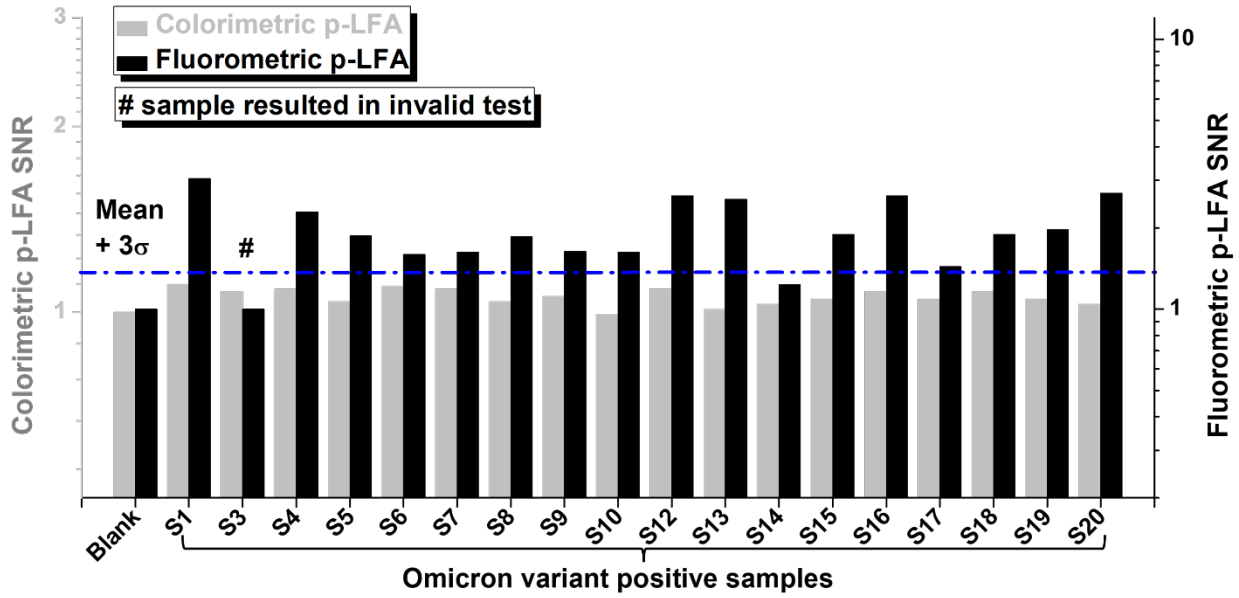

Supplementary Fig. 27 l N-protein signal-to-noise ratio in PCR-positive Omicron BA.1 variant NP swab samples determined by colorimetric p-LFA (gray bars) and fluorometric p-LFA (black bars).

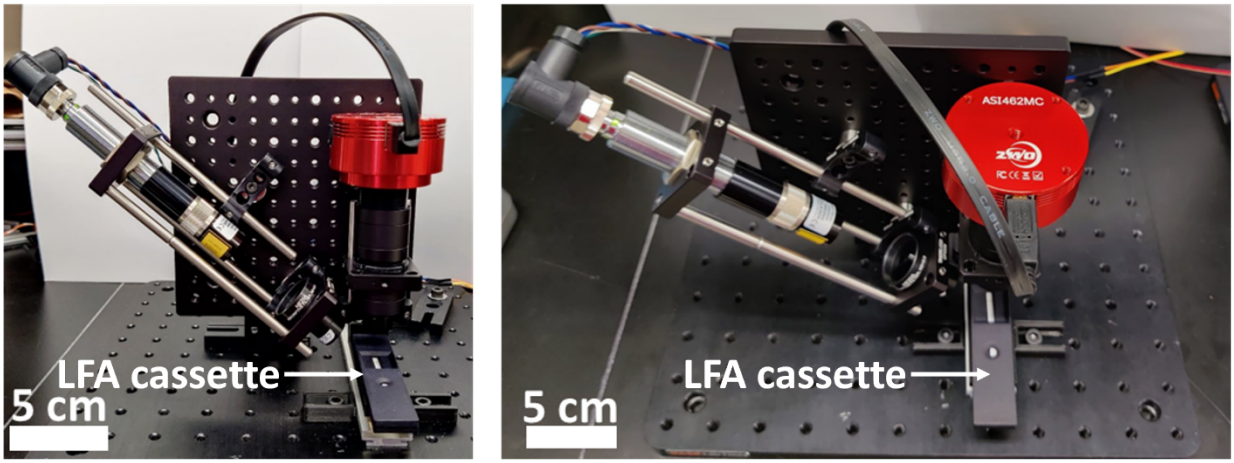

Supplementary Fig. 28 l Photograph of the portable fluorescence scanner for different angle. The size of the scanner is 25 cm x 25 cm x 19 cm (LxBxH).

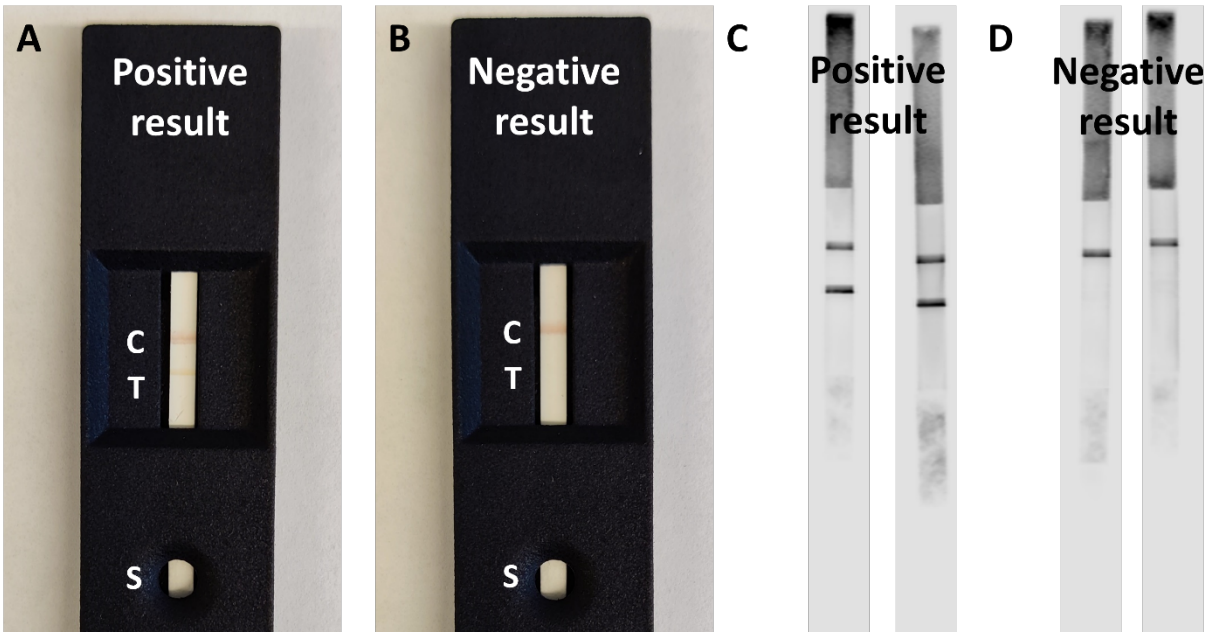

Supplementary Fig. 29 l Photographs of LFA cassette employed in the study**.** S, C and T corresponds to the sample pad, test line and control line, respectively. Representative photographs of LFA cassette displaying **(A)** positive and **(B)** negative result from p-LFA strips with colorimetric control line. Representative fluorescence images of the p-LFA strips displaying **(C)** positive and **(D)** negative result from p-LFA strips with fluorometric control line.

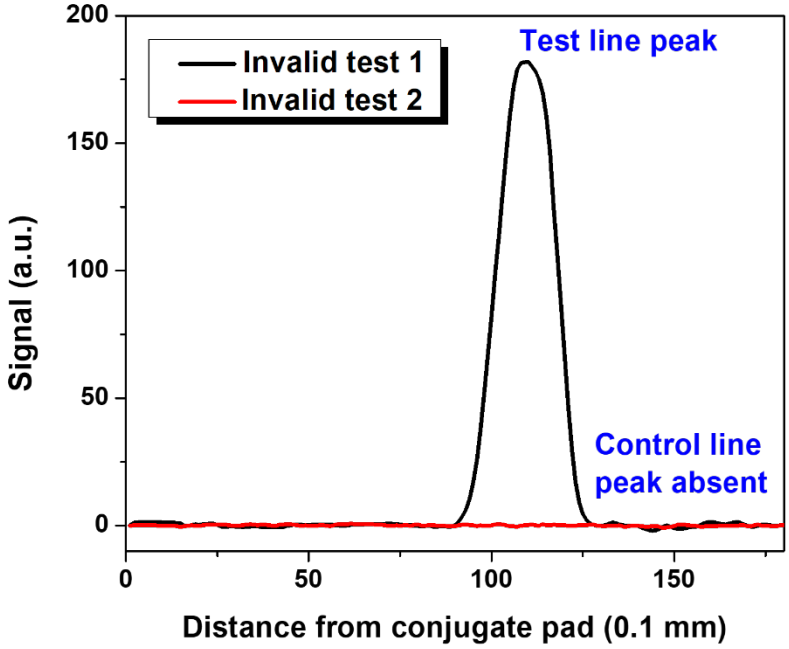

Supplementary Fig. 30 l Representative invalid tests obtained using the portable scanner. If a test has no signal at the control line, it is reported as an invalid test.

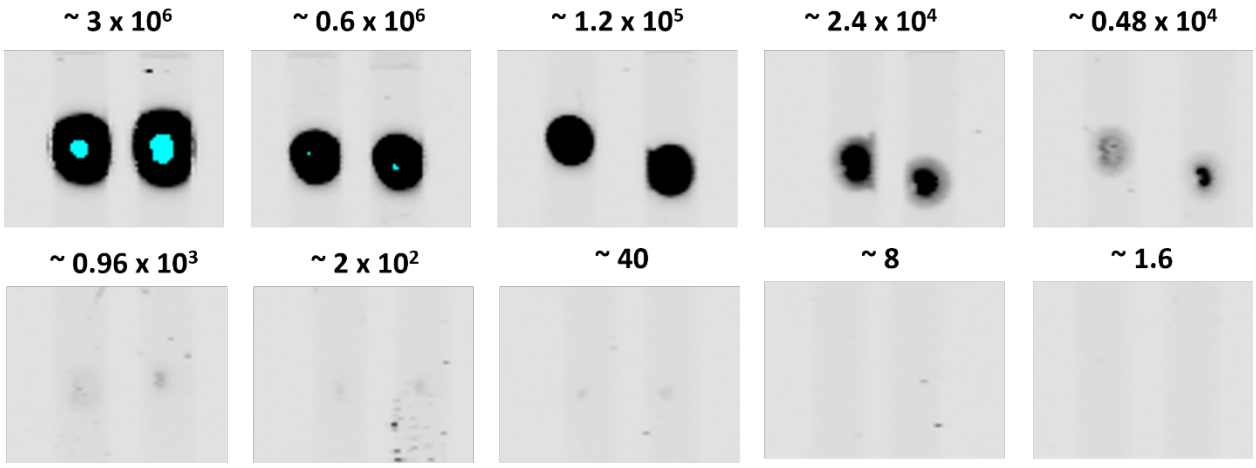

Supplementary Fig. 31 l Fluorescence images of the LFA strips drop-casted with 0.5 μl of different numbers of plasmonic-fluors (mentioned in parenthesis).

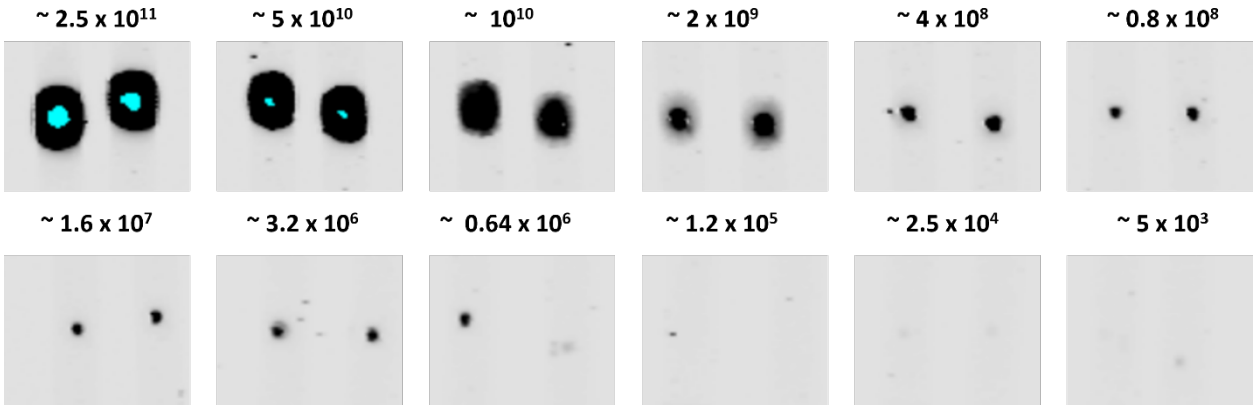

Supplementary Fig. 32 l Fluorescence images of the LFA strips drop-casted with 0.5 μl of different concentrations of molecular-fluorophores (mentioned in parenthesis).

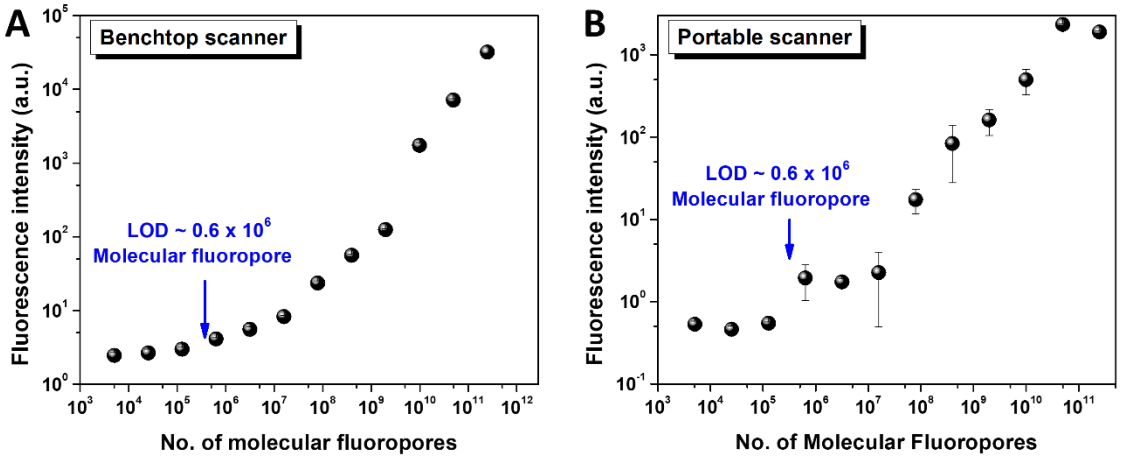

Supplementary Fig. 33 l (A) Fluorescence intensities and **(B)** area under the curve values obtained from LFA strips, drop-casted with different concentrations of molecular fluorophores, when scanned using benchtop (LI-COR) and portable scanner, respectively.

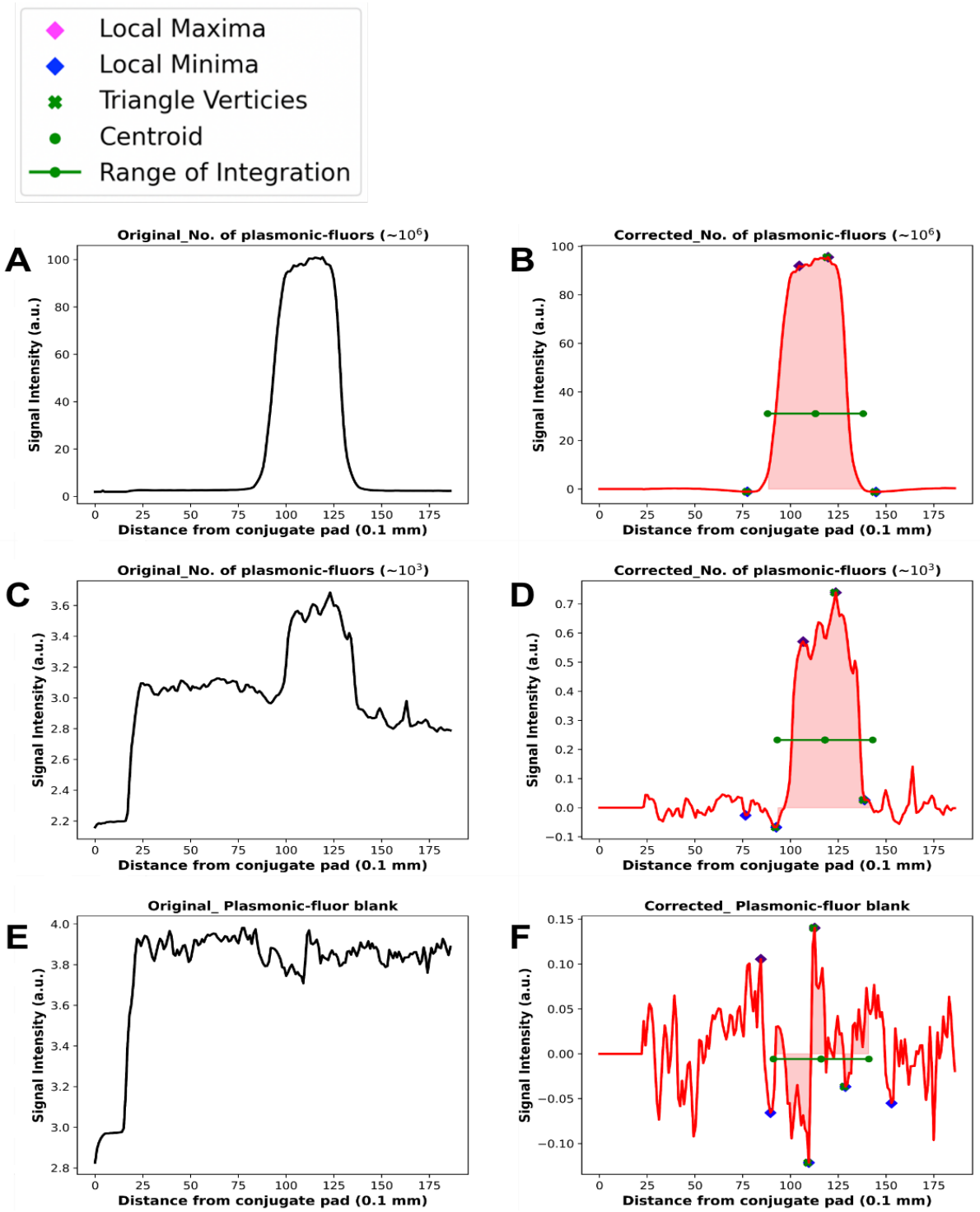

Supplementary Fig. 34 l Representative examples of data processing conducted on data acquired by portable scanner from LFA strips drop-casted with **(A, B)** ~10^6 and **(C, D)** ~10^3 number of plasmonic-fluors, and **(E, F)** 1XPBS (blank).

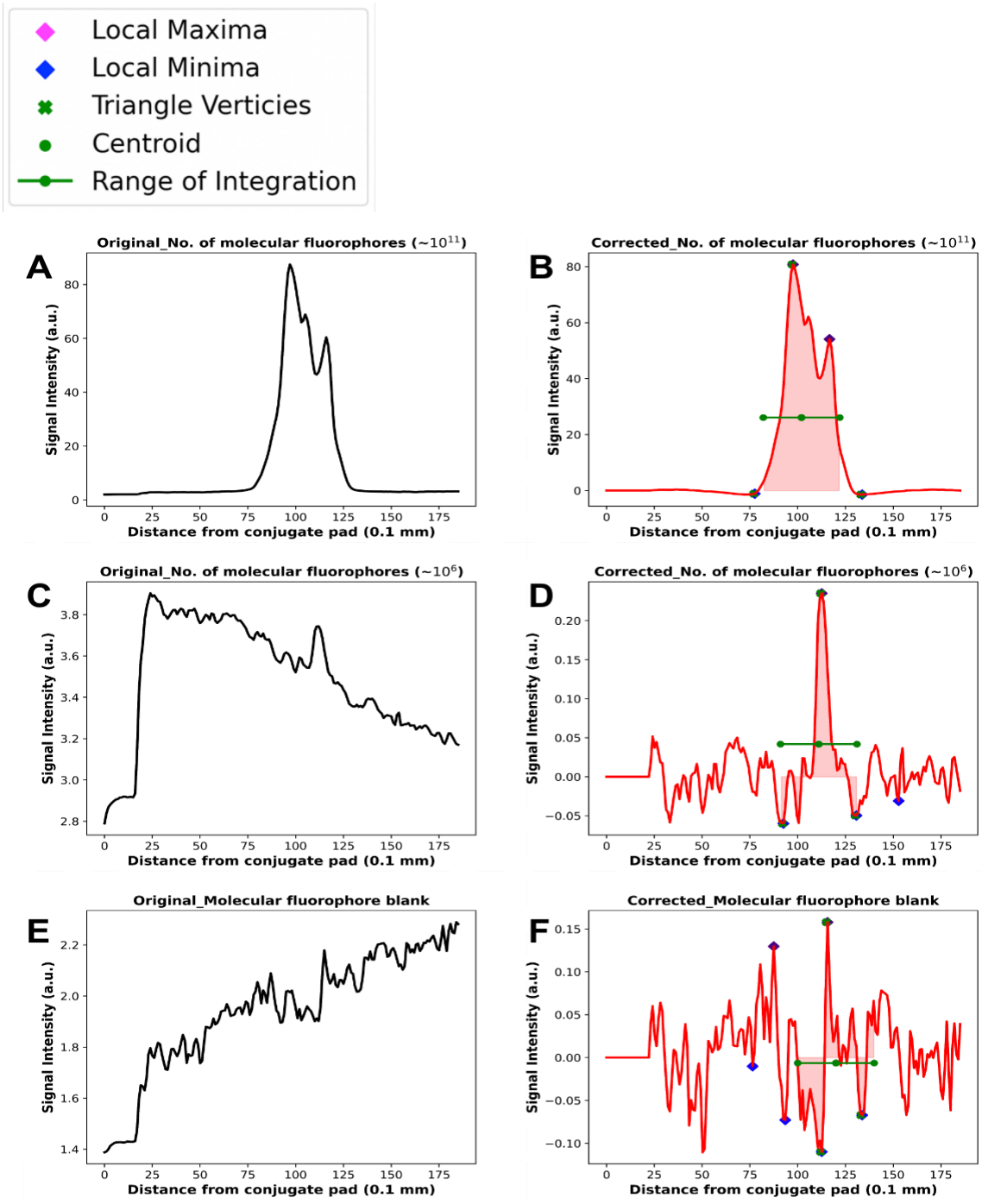

Supplementary Fig. 35 I Representative examples of data processing conducted on data acquired by portable scanner from LFA strips drop-casted with **(A, B)** ~10^{11} and **(C, D)** ~10^{6} number of molecular fluorophores, and **(E, F)** 1XPBS (blank).

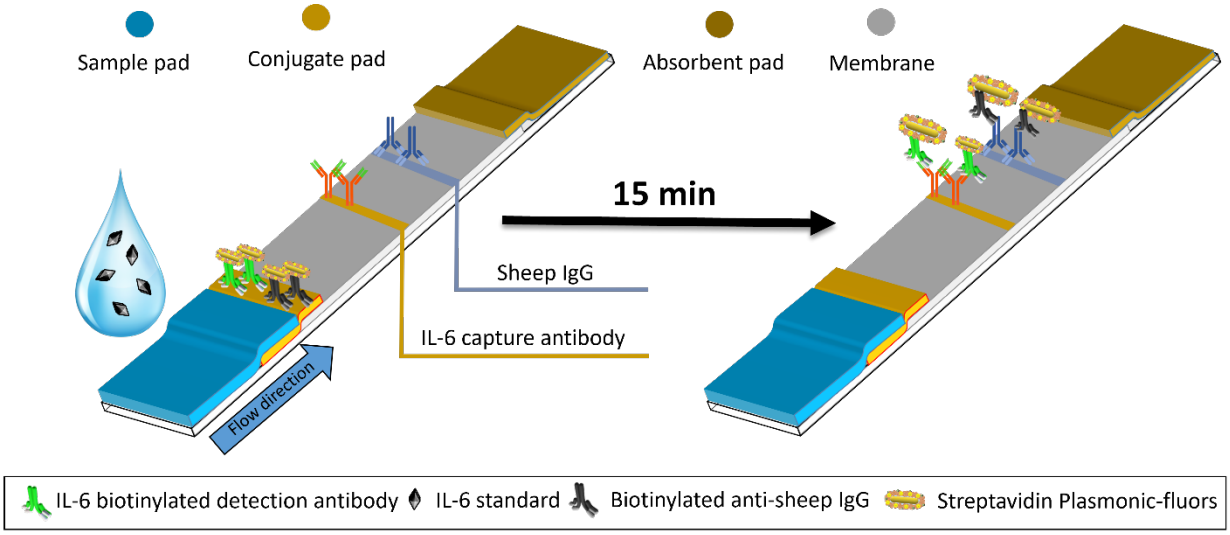

Supplementary Fig. 36 l Schematic illustration of the full-strip 15 min IL-6 p-LFA employing plasmonic-fluors as nanolabel for both control and test lines.

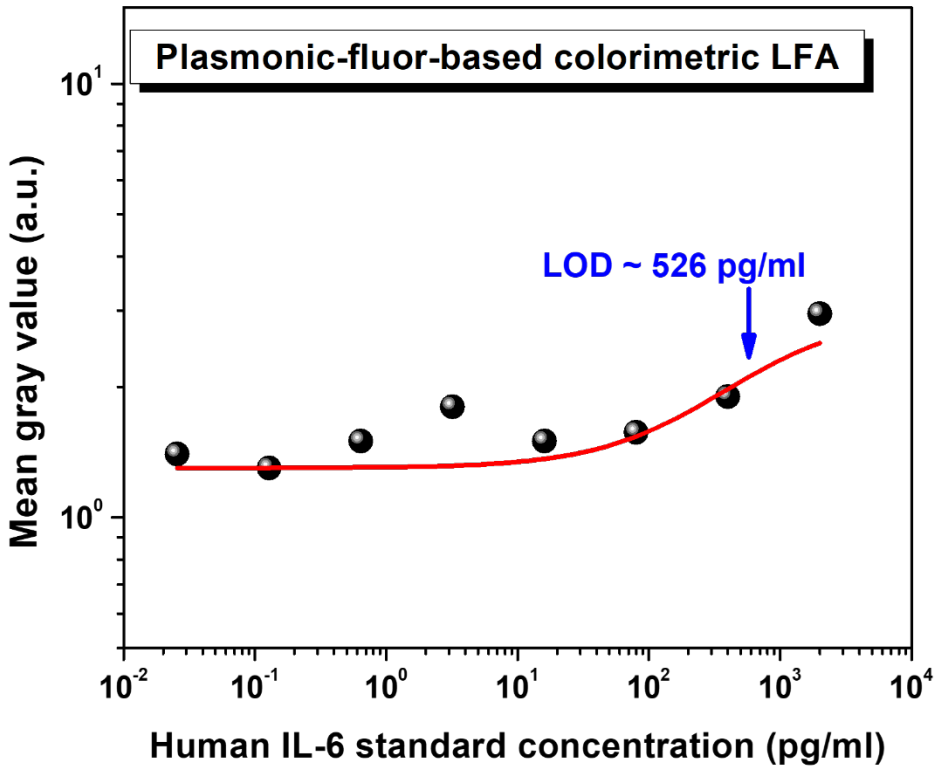

Supplementary Fig. 37 l Dose-dependent mean gray values obtained from test line of the nitrocellulose membrane corresponding to different concentrations of IL-6 solutions acquired from plasmonic-fluor-based IL-6 LFA.

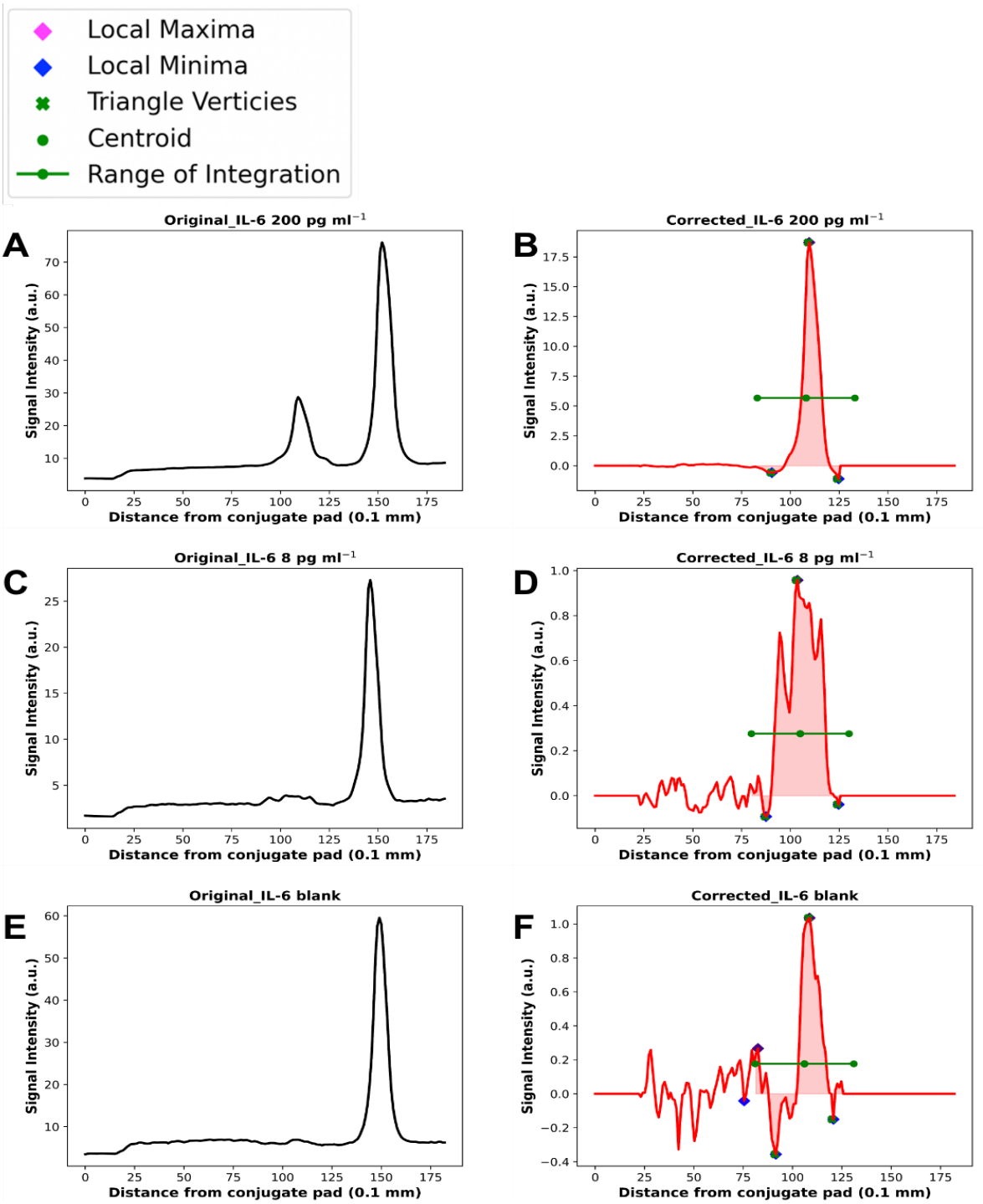

Supplementary Fig. 38 l Representative examples of data processing conducted on data acquired by portable scanner from IL-6 p-LFA strips exposed to **(A, B)** 200 and **(C, D)** 1.6 pg ml^{-1} concentration of IL-6 standard, and **(E, F)** 1XBSA 1%BSA (blank).

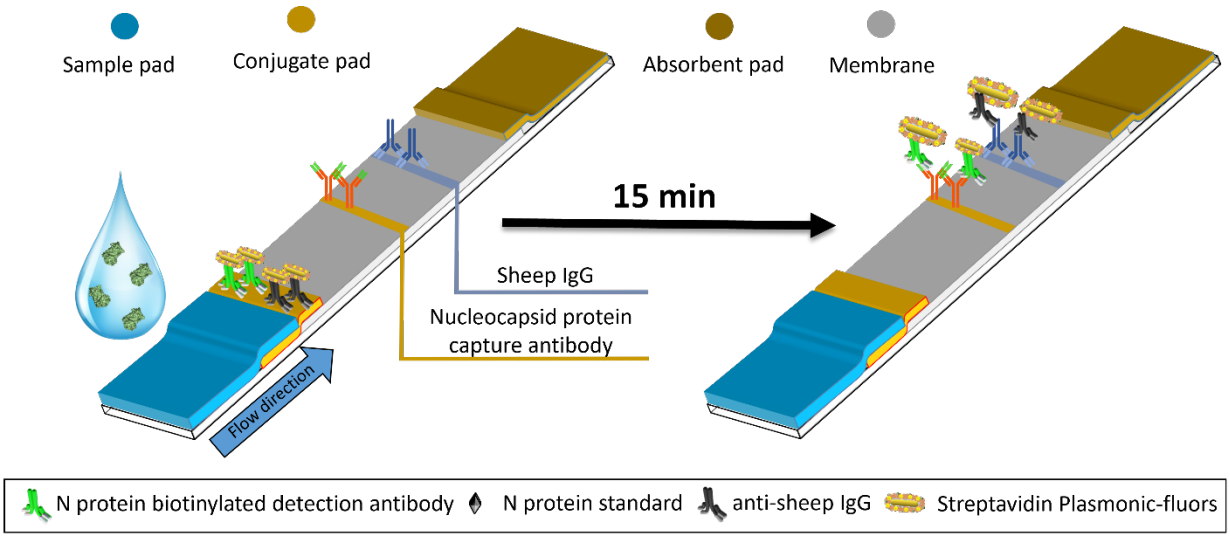

Supplementary Fig. 39 l Schematic illustration of the full-strip 15 min N protein p-LFA employing plasmonic-fluors as nanolabel for both control and test lines.

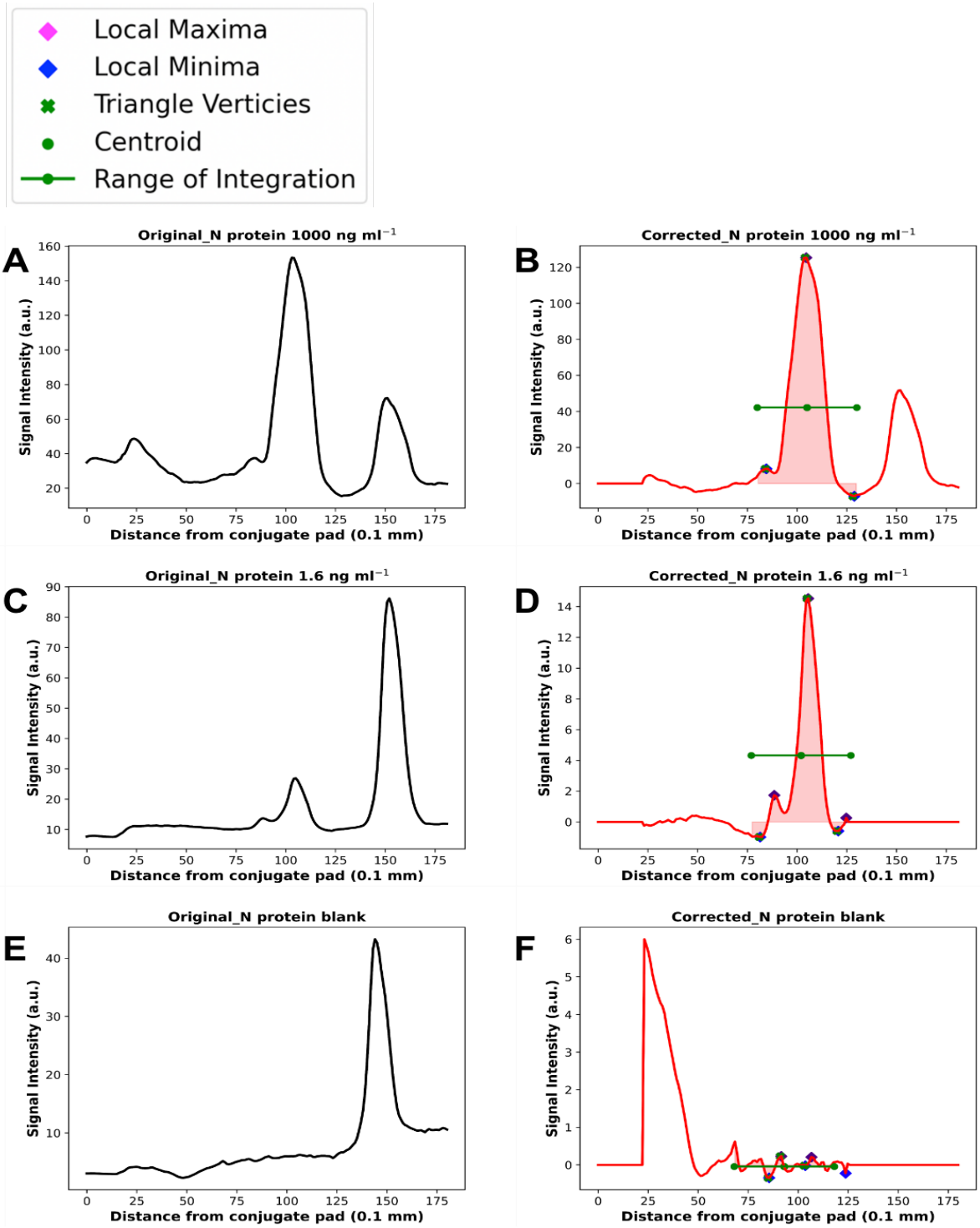

Supplementary Fig. 40 l Representative examples of data processing conducted on data acquired by portable scanner from N protein p-LFA strips exposed to **(A, B)** 1000 and **(C, D)** 1.6 ng ml^{-1} concentration of N protein standard, and **(E, F)** 1XBSA 1%BSA (blank).

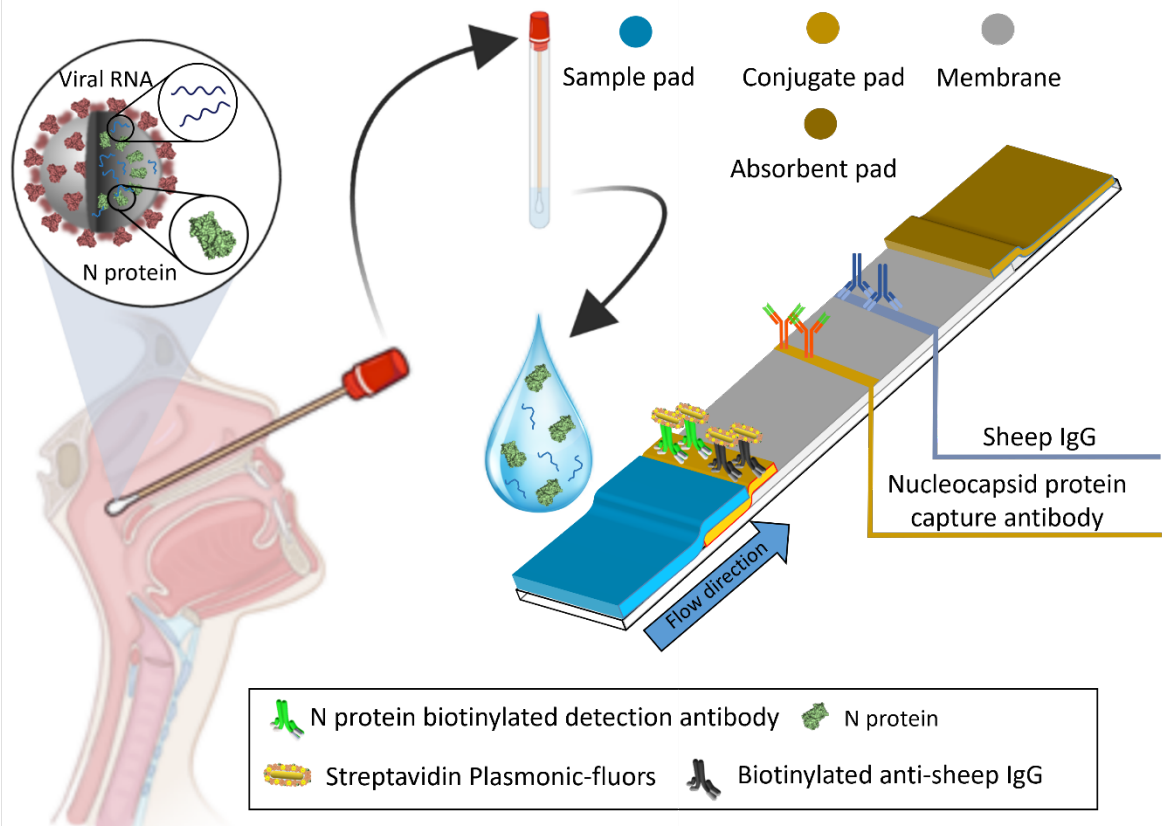

Supplementary Fig. 41 l Schematic illustration of the full strip N protein p-LFA employed for the quantitative measurement of N protein concentration present in the nasal swab samples of COVID-19 positive (PCR confirmed) individuals.

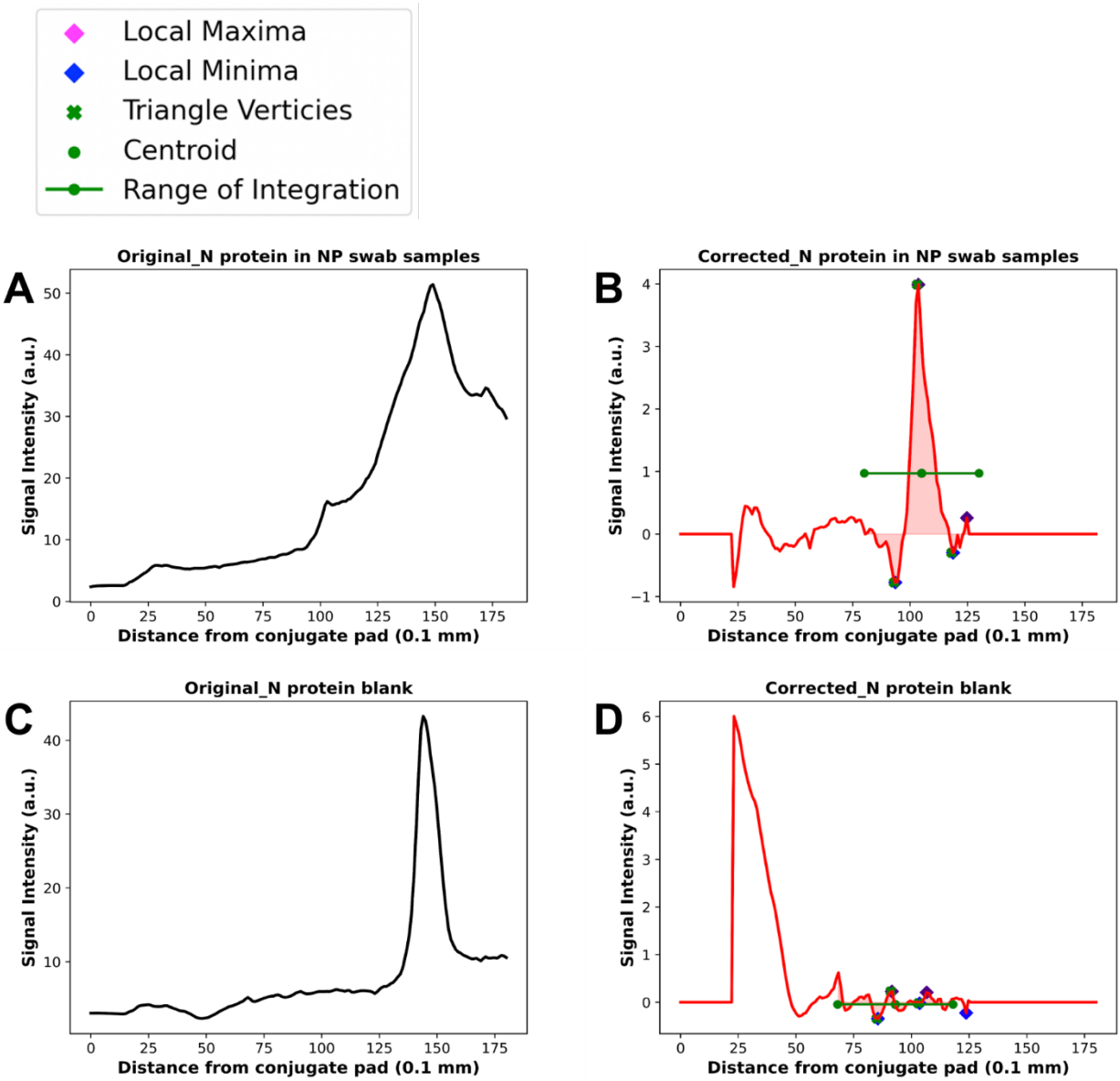

Supplementary Fig. 42 l Representative examples of data processing conducted on data acquired by portable scanner from N protein p-LFA strips exposed to the **(A, B)** nasal swab sample of the PCR-positive individuals and **(C, D)** blank for quantitative analysis of N protein concentration.

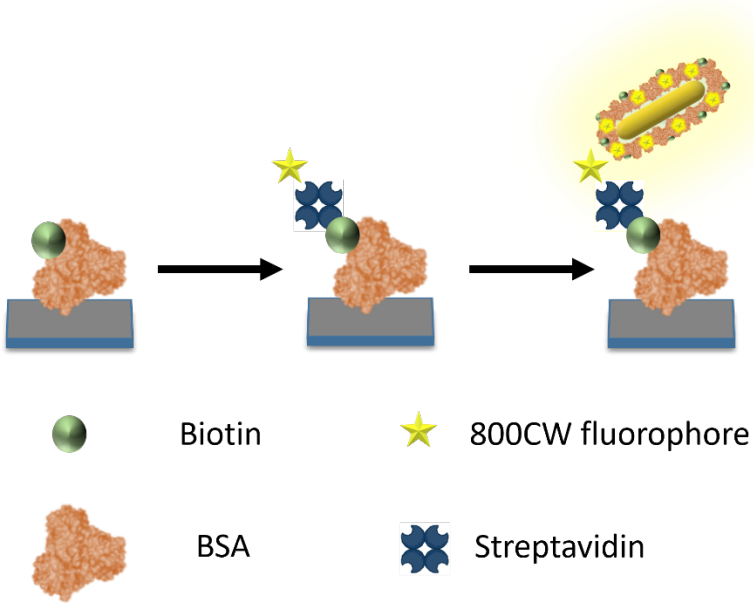

Supplementary Fig. 43 l Schematic illustration of experiment designed to understand the enhancement of fluorescence signal using plasmonic-fluors compared to conventional fluorophores.

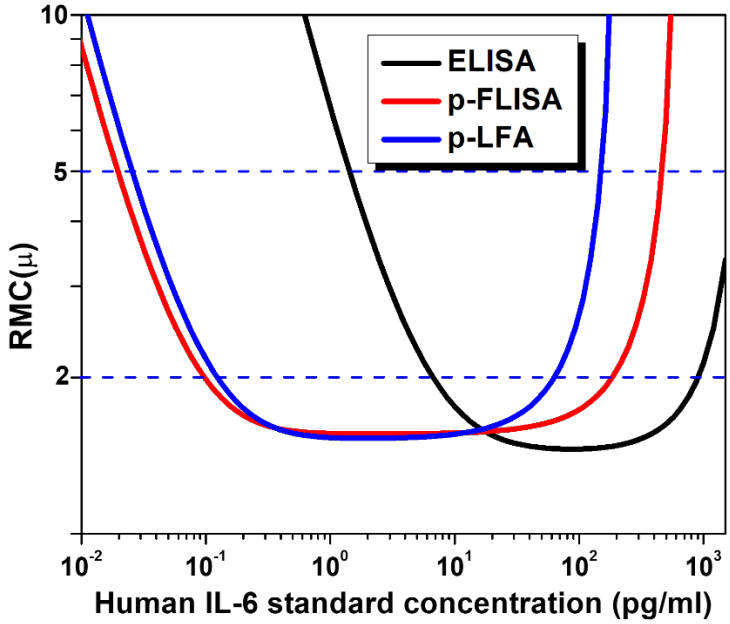

Supplementary Fig. 44 l RMC curves for ELISA, p-FLISA and p-LFA calculated via equations listed in supplementary information. The blue dashed line indicates the RMC cutoffs that can be used to determine the quantitative performance of the assay over a certain range of concentrations. The relevant RMC parameters are listed in Supplementary table 1.

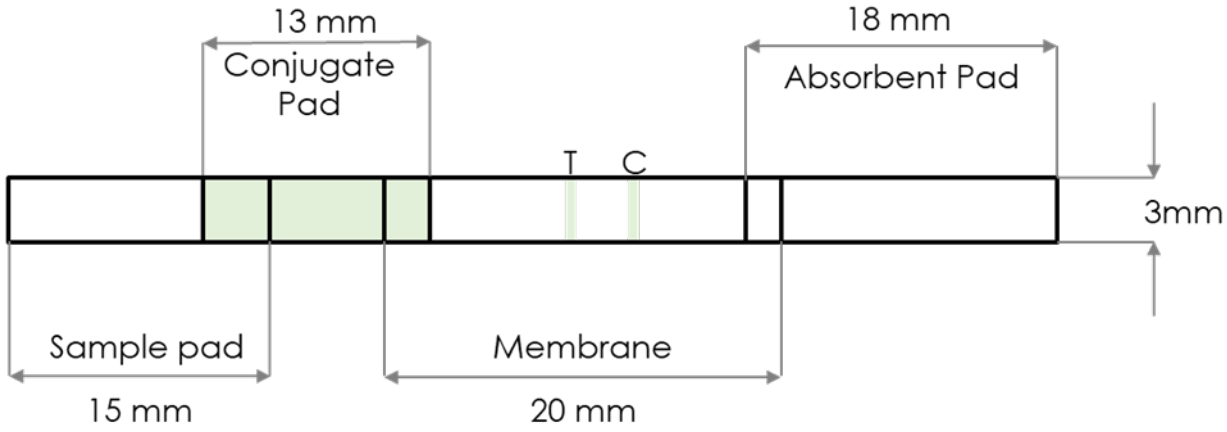

Supplementary Fig. 45 l Schematic illustration of assembly of LFA components. The prepared sample pad, conjugate pad, membrane, and adsorption pad were then assembled with a 2 mm overlap between each pad and cut to strips with a width of 3mm using a strip cutter.

Supplementary Table 1 l RMC function and bioanalytical parameters of human IL-6 ELISA, p-FLISA and p-LFA to compare the performance of the assays in terms of their ability to resolve.

Parameter	ELISA	p-FLISA	p-LFA
μ_{min}	1.46	1.56	1.45
Concentration at μ_{min} (pg ml^{-1})	83.43	1.99	2.47
Range of $\mu < 2$ (pg ml^{-1})	6.71–900.9	0.1–184.1	0.13–86.08
Range of $\mu < 5$ (pg ml^{-1})	1.42–1762	0.02–463.8	0.03–181
Limit-of-detection (pg ml^{-1})	2900	0.016	0.093
Limit-of-quantitation (pg ml^{-1})	9100	0.058	0.298

Supplementary Table 2 l Table depicting the clinical sensitivity and specificity of the SARS-CoV-2 S1 antibody p-LFA.

	ELISA IgG positive samples	Pre-COVID samples
Sample quantity	**79**	**48**
LFA IgG positive	**76**	**0**
Sensitivity*	**96.2%**	
Specificity	**100%**	

Supplementary Table 3 l Details of the 19-PCR positive patient samples.

Sample #	Age	Comorbidities*	Duration of symptoms (days)	Symptoms	Radiographic findings at diagnosis/testing: Chest X-ray (CXR) or Computed Tomography (CT) imaging	Severity/Critical illness/ Intensive care requirement
S1	33	Asthma	4	Chest pain and constipation- nonspecific symptoms.	clear lungs	nil
S2	57	none	7	Shortness of breath, Hypoxic Treated with remdesivir	Bilateral (b/l) interstitial infiltrates s/o viral pneumonia	nil
S3	49	none	14	Flu like symptoms 2 weeks ago.	CT chest : Interstitial thickening and parenchymal infiltrates	nil
S4	59	none	3	Cough malaise, Shortness of breath x 3 days, Hypoxia+	b/l lower lobe infiltrates.	ICU admit for seizure unrelated to COVID
S5	62	COPD	2	Shortness of breath.	clear lungs	nil
S6	77	HTN, CKD	1	Shortness of breath.	b/l lower lobe infiltrates	Non – invasive ventilation, ICU admit
S7	27	Psychosis	asymptomatic	None. COVID PCR + 2 weeks prior	clear lungs	nil
S8	55	HIV (poorly controlled)	14	Cough, Shortness of breath 2 weeks. Hypoxia+	left lower pneumonia	nil
S9	53	ESRD, DM	2	Shortness of breath, Fever, Loss of taste.	b/l diffuse interstitial opacity	nil
S10	37	none	asymptomatic	Presurgical screening. Tibial fracture	clear lungs	nil
S11	71	DM	3	Loss of taste, Malaise, Shortness of breath	Patchy consolidation b/l	nil

S12	41	DM	3	Chest pain- diagnosed as costochondritis.	clear lungs	nil
S13	58	DM	3	Flu like illness, fever, myalgia	clear lungs	nil
S14	69	DM, CAD	3-5	Few days flu like symptoms,	b/ll diffuse interstitial opacities	ICU admit Ventilated for hypoxic respiratory failure. Died
S15	44	none	14	Cough, Shortness of breath for 2 weeks	clear lungs	nil
S16	70	none	2	Fever, Cough, Shortness of breath	b/l mild interstitial opacities	nil
S17	61	HTN	6	Cough, Shortness of breath	b/l interstitial and airspace opacities	nil
S18	42	Obesity CHF	2	Shortness of breath, cough, diarrhea, and myalgias	Multifocal PNA	ICU admit. Increase from home vent settings
S19	47	COPD	7	Shortness of breath.	clear lungs	nil

*DM= diabetes mellitus, COPD= chronic obstructive pulmonary disease, ESRD = End stage renal disease, HIV= human immunodeficiency virus infected, CHF= congestive heart failure, CAD coronary heart disease

Supplementary Table 4 l Results of the 19 PCR-positive patient samples (wild type SARS-CoV-2) tested by fluorometric and colorimetric p-LFA, and commercial antigen test (BD veritor™). Table also lists the N protein concentration of these samples obtained from fluorometric p-LFA demonstrating its quantitative analysis ability.

Sample #	CT value (average of 2 tests)	p-LFA fluorometric result (concentration in ng/ml)	P-LFA colorimetric result (concentration in ng/ml)	FDA-approved BD veritor™ (commercial antigen kit) result
S1	40.7	Positive (20.58)	Negative	Negative
S2	19.2	Positive (5.75)	Negative	Positive
S3	27.9	Positive (58.93)	Positive (below LOQ)	Negative
S4	30.5	Negative	Negative	Negative
S5	42.8	Positive (54.72)	Positive (below LOQ)	Negative
S6	22.6	Positive (6.93)	Negative	Positive
S7	39.5	Positive (4.93)	Negative	Negative
S8	21.8	Positive (856)	Positive (570.6)	Positive
S9	18.2	Positive (222)	Positive (292.3)	Positive
S10	36.3	Positive (1.49)	Negative	Negative
S11	18.8	Positive (2.45)	Negative	Positive
S12	39.5	Positive (213.9)	Positive (268.6)	Negative
S13	20.7	Positive (73.12)	Positive (below LOQ)	Positive
S14	23.8	Positive (160.3)	Positive (below LOQ)	Negative
S15	32.7	Positive (8.09)	Negative	Negative
S16	29.3	Positive (112.6)	Positive (below LOQ)	Negative
S17	27.8	Positive (2.31)	Negative	Positive
S18	23.5	Positive (27.47)	Negative	Positive
S19	42.3	Positive (7.1)	Negative	Negative

Supplementary Table 5 l Results of the 16 PCR-positive Delta B.1.617.2 variant samples (confirmed by gene sequencing) tested using fluorometric and colorimetric p-LFA. Table also lists the N protein concentration of these samples obtained from fluorometric p-LFA demonstrating its quantitative analysis ability.

Sample #	CT value 1	CT value 2	p-LFA fluorometric result (concentration in ng/ml)	p-LFA colorimetric result (concentration in ng/ml)
D1	20.26	20.09	Positive (44.63)	Negative
D2	22.5	24.3	Positive (358.6)	Positive (299.3)
D3	24.8	26.8	Positive (367.5)	Positive (233.9)
D4	25.02	25.15	Positive (1.81)	Negative
D5	22.6	24.3	Positive (348.1)	Positive (268.2)
D6	23.1	24.8	Positive (2.51)	Negative
D7	20.7	22.5	Positive (135.7)	Positive (below LOQ)
D8	18.4	20.1	Positive (63.17)	Positive (below LOQ)
D9	13.3	14.2	Positive (43.56)	Negative
D10	17.98	18.17	Positive (124.5)	Positive (below LOQ)
D11	15.25	15.17	Positive (3.18)	Negative
D12	18.86	18.85	Positive (2.66)	Negative
D13	22.56	22.23	Positive (29.39)	Negative
D14	15.24	15.08	Positive (below LOQ)	Negative
D15	17.59	16.95	Positive (120)	Positive (below LOQ)
D16	15.9	15.44	Positive (19.05)	Negative

Supplementary Table 6 l Results of the 17 PCR-positive omicron BA.1 samples (confirmed by gene sequencing) tested using fluorometric and colorimetric p-LFA. Table also lists the N protein concentration of these samples obtained from fluorometric p-LFA demonstrating its quantitative analysis ability.

Sample #	CT value 1	CT value 2	p-LFA fluorometric result (concentration in ng/ml)	p-LFA Colorimetric Result
O1	19.22	19.19	Positive (3.74)	Negative
O3	18.32	17.45	Invalid test (control line was not visible)	Negative
O4	19.59	19.28	Positive (1.76)	Negative
O5	18.51	18.25	Positive (below LOQ)	Negative
O6	17.71	17.54	Positive (below LOQ)	Negative
O7	18.81	18.42	Positive (below LOQ)	Negative
O8	20.04	19.98	Positive (below LOQ)	Negative
O9	18.56	18.17	Positive (below LOQ)	Negative
O10	19.08	18.28	Positive (below LOQ)	Negative
O12	18.93	18.53	Positive (2.35)	Negative
O13	19.11	18.51	Positive (2.2)	Negative
O14	18.69	18.42	Positive (below LOQ)	Negative
O15	20.22	19.66	Positive (0.99)	Negative
O16	20.41	19.84	Positive (2.54)	Negative
O17	18.77	18.2	Positive (below LOQ)	Negative
O18	17.94	17.53	Positive (0.99)	Negative
O19	19.97	19.95	Positive (1.13)	Negative
O20	18.2	17.71	Positive (2.71)	Negative

Supplementary Table 7 l Details of 17 PCR-positive omicron BA.1 samples (confirmed by gene sequencing).

Sample #	Age	Comorbidities*	Duration of symptoms (days)	Symptoms	Radiographic findings at diagnosis/testing: Chest X-ray (CXR) or Computed Tomography (CT) imaging	Severity/Critical illness/ Intensive care requirement
S1	82		2	Cough, Runny nose	NA	No
S3	34		2	Fever, Runny nose	NA	No
S4	35		1	Sore throat, Diarrhea	NA	No
S5	30		2	Fever; Cough; Muscle Aches	NA	No
S6	52		1	Cough, Sore throat	NA	No
S7	38		2	Fever,Cough,Sore throat	NA	No
S8	57		1	Fever, Cough	NA	No
S9	50		1	Cough	NA	No
S10	26		2	Chills, Nasal Congestion	NA	No
S12	28		2	Cough Headache, Nasal congestion	NA	No
S13	63		1	Headache, Nasal congestion	NA	No
S14	51		1	Fever, Runny nose	NA	No
S15	39		1	Cough	CXR : Normal	No
S16	27		1	Cough, Sore throat	NA	No
S17	46		1	Cough, Sore throat	NA	No
S18	25		2	Cough, Fever, Muscle aches	NA	No
S19	81	ESRD Lung cancer	2(9)	Cough,Dyspnea	CXR: Multifocal Pneumonia	Moderate disease (tested 9 days ago negative)
S20	30		2	Headache, Nasal congestion	NA	No

Supplementary Table 8 l N protein concentration determined by p-LFA strips and measured by portable and benchtop scanner.

Sample #	N protein conc. determined by p-LFA and measured by portable scanner	N protein conc. determined by p-LFA and measured by benchtop scanner
S3	36.09	55.62
S5	41.65	51.81
S8	216	259
S9	184.3	201.1
S12	154.6	197.2
S13	67.18	62.12
S14	101.2	154.9
D2	268.6	325.5
D3	253.7	329.5
D5	267.7	315.1
D7	138	113.7
D8	105.8	53.26
D10	97.9	112.6
D15	129	110.9

Supplementary Table 9 l IL-6 concentration determined by p-LFA strips and measured by portable and benchtop scanner; and determined by p-FLISA and measured by benchtop scanner.

Sample #	IL-6 conc. (pg/ml) determined by p-LFA and measured by portable scanner	IL-6 conc. (pg/ml) determined by p-LFA and measured by benchtop scanner	IL-6 conc. (pg/ml) determined by p-FLISA and measured by benchtop scanner
1	213.5	245.5	359.5
2	65.54	88.3	46.97
3	125.2	99.79	108.8
4	18.57	28.96	8.75
5	12.72	16.74	1.61
7	39.31	29.11	33.87
8	66.75	52.13	161
9	66.96	80.88	24.94
10	55.65	75.74	69.25
11	58.93	42.50	82.95
12	58.95	52.89	60.21
13	87.02	48.71	51.89
14	11.66	7.31	60.07
15	30.07	45.16	34.47
17	56.75	46.51	63.01
18	19.92	29.5	28.35
19	326.6	383.4	17.31
21	489.3	337.5	549.4
22	953.2	1046	1003
23	302.4	379.2	119.9
24	36.24	27.91	61.91
25	602.1	749.5	746.3
26	168	198.9	125.2
27	101.4	67.92	97.06
28	61.73	45.75	12.01
29	56.98	41.42	99.58
30	70.45	101.7	16.73
32	348.3	293.1	516.5

References:

1. Gupta, R.; Luan, J.; Chakrabartty, S.; Scheller, E. L.; Morrissey, J.; Singamaneni, S., Refreshable Nanobiosensor Based on Organosilica Encapsulation of Biorecognition Elements. *ACS applied materials & interfaces* **2020,** *12* (5), 5420-5428.
2. Luan, J.; Seth, A.; Gupta, R.; Wang, Z.; Rathi, P.; Cao, S.; Derami, H. G.; Tang, R.; Xu, B.; Achilefu, S., Ultrabright fluorescent nanoscale labels for the femtomolar detection of analytes with standard bioassays. *Nature biomedical engineering* **2020,** *4* (5), 518-530.
3. Tebbe, M.; Kuttner, C.; Männel, M.; Fery, A.; Chanana, M., Colloidally stable and surfactant-free protein-coated gold nanorods in biological media. *ACS applied materials & interfaces* **2015,** *7* (10), 5984-5991.
4. Wilson, B. D.; Eisenstein, M.; Soh, H. T., Comparing assays via the resolution of molecular concentration. *Nature Biomedical Engineering* **2022,** *6* (3), 227-231.
5. Harris, C. R.; Millman, K. J.; Van Der Walt, S. J.; Gommers, R.; Virtanen, P.; Cournapeau, D.; Wieser, E.; Taylor, J.; Berg, S.; Smith, N. J., Array programming with NumPy. *Nature* **2020,** *585* (7825), 357-362.
6. Hunter, J. D., Matplotlib: A 2D graphics environment. *Computing in science & engineering* **2007,** *9* (03), 90-95.
7. Zhao, J.; Lui, H.; McLean, D. I.; Zeng, H., Automated autofluorescence background subtraction algorithm for biomedical Raman spectroscopy. *Applied spectroscopy* **2007,** *61* (11), 1225-1232.
8. de Rooi, J. J.; Eilers, P. H., Mixture models for baseline estimation. *Chemometrics and Intelligent Laboratory Systems* **2012,** *117*, 56-60.
9. Virtanen, P.; Gommers, R.; Oliphant, T. E.; Haberland, M.; Reddy, T.; Cournapeau, D.; Burovski, E.; Peterson, P.; Weckesser, W.; Bright, J., SciPy 1.0: fundamental algorithms for scientific computing in Python. *Nature methods* **2020,** *17* (3), 261-272.